Norwegian University of Life Sciences
Faculty of of Mathematics, Nature and Science
Department of Chemistry, Biotechnology and
Food Science

Master Thesis 2015
60 credits

# Identification and Validation of a Novel Biomarker for Tankyrase Inhibition in Selected Carcinoma Cells

Aisha Rehman Moghal

# Table of contents

# Acknowledgements

The work presented in this master thesis was carried out at the Unit for Cell Signaling (Department of Microbiology, Oslo University Hospital) in the period from January 2014 to January 2015.

I am extremely grateful to Professor Stefan Krauss for giving me the opportunity to work in his wonderful group and for reading and constructive criticism of this thesis. Furthermore, I am truly grateful to my supervisor, Jo Waaler, for excellent guidance and support throughout the year. I would also like to thank Line Mygland for all the practical help in the execution of the cell culturing and cell proliferation assays.

I would also like to express my gratitude to Petter Angell Olsen, Nina Therese Solberg, Kaja Lund and Tore Vehus for reading my thesis and a great social environment.

I would also like to thank Janne Beate Utåker from Norwegian University of Life Sciences for being a wonderful advisor throughout my master studies. Thanks also to Professor Tor Lea from Norwegian University of Life Sciences for good advices during this thesis.

Thanks to my sister, Mariam Zubair, for reading the thesis. Thanks to my husband, Abdul Rehman Moghal, and my daughter, Amna, for taking care of my little angel, Arifa, so that I could work in peace. Thanks to my parents and entire family for believing in me that I will manage. Love you all.

Oslo, February 2015

Aisha Rehman Moghal

# Abstract

Tankyrase is a key regulator of cell signaling and metabolism [1]. Tankyrase is a catalytic enzyme that modifies protein turn-over through a post translational modification called poly(ADP)-ribosylation [1]. One of the central target proteins of tankyrase mediated poly(ADP)-ribosylation is AXIN1/2 that regulate the canonical WNT/β-catenin pathway [1][2][3]. Tankyrase inhibition leads to reduced cell growth accompanied with reduced levels of β-catenin, the key mediator of the canonical WNT/β-catenin pathway, in selected cancer cell lines [3][4]. However, in several other cancer cell lines, growth reduction by tankyrase inhibition appears to be independent of altered canonical WNT/β-catenin pathway activity [4].

With the aim of identifying a more general biomarker for tankyrase inhibition, 660 tumor cell lines were screened for sensitivity to the novel tankyrase inhibitor G007-LK. Among the cancer cell lines that exhibited growth alteration in response to G007-LK treatment, five cell lines were selected for further analysis: ABC-1, a non-small-cell lung cancer cell line; OVCAR-4, an ovarian cancer cell line; A-498, a renal cancer cell line; COLO320DM and SW480, both colon cancer cell lines.

An expression profile analysis revealed B-cell lymphoma 2 modifying factor (*BMF*) to be strongly upregulated in the highly G007-LK sensitive cell line ABC-1. This upregulation was not accompanied with altered *AXIN2* mRNA expression, a hallmark of canonical WNT signaling [5]. We found that *BMF* transcription, was upregulated in ABC-1, COLO320DM, OVCAR-4 and SW480 cells at 24 and 72 hours after exposure to 1 μM of the tankyrase inhibitor G007-LK (Fig. 3-2A). In A498 cells, an upregulation of *BMF* transcripts was only observed at 24 hours (Fig. 3-2A). The upregulation of *BMF* was accompanied with a down-regulation of *AXIN2* transcription in COLO320DM, OVCAR-4 and SW480 cells (Fig. 3-2A). All selected cancer cell lines show AXIN1 protein stabilization upon tankyrase inhibition at 72 h of G007-LK treatment, while only SW480 and COLO320DM also show a clear down-regulation of β-catenin (Fig. 3-2B, 3-4B).

AMPK-activation has been implicated in the activation of *BMF* transcription [6] and upregulated phosphorylated-AMPKα (Thr172) protein levels display AMPK activation [7]. We were not able to detect alterations in phosphorylated-AMPKα (Thr172) protein levels in G007-LK treated ABC-1 cells (Fig. 3-3B). Also in COLO320DM cells, total APMKα protein levels were unaltered by tankyrase inhibition, but phosphorylated AMPKα (Thr172) protein levels were substantially raised upon 72 h of G007-LK exposure (Fig. 3-4B, right). In contrast, total AMPKα levels were reduced by tankyrase inhibition in *BMF* depleted COLO320DM cells, compared to cells treated with *BMF* esiRNA. However, increased phosphorylated AMPKα (Thr172) protein levels were still seen. In conclusion, tankyrase inhibition affected AMPKα protein levels only in the absence of *BMF*, again compared to cells treated with *BMF* esiRNA. However, G007-LK increased phosphorylated AMPKα (Thr172) protein levels independent of *BMF* (Fig. 3-4B, right).

To sum up: (i) We established *BMF* transcripts as potentially broader biomarkers for tankyrase inhibition in cancer cells compared to the previously used β-catenin biomarker (Fig. 3-2A, 3-2B), (ii) we show a regulatory interaction between *BMF* and AMPKα in COLO320DM that depends on tankyrase inhibitor G007-LK activity (Fig. 3-4B, right) and (iii) we finally demonstrate that AMPK phosphorylation (at Thr172) is increased by G007-LK-mediated TNKS1/2 inhibition, perhaps through AXIN1 stabilization, in COLO320DM (Fig. 3-4B, right).

# Sammendrag

Tankyrase er en svært viktig regulator av signaltransduksjon og metabolisme i celler [1]. Tankyrase er et katalytisk enzym som modifiserer proteiners nedbryting via den posttranslasjonelle modifiseringen poly(ADP)-ribosylering [1]. Et av de viktigste proteinene som poly(ADP)-ribosyleres av tankyrase er AXIN1/2, to proteiner som igjen regulerer aktiviteten til WNT/β-catenin-signalveien [1][2][3]. I et utvalg av kreftceller fører hemming av tankyrase til redusert cellevekst parallelt med reduserte nivåer av β-catenin som er WNT/β-catenin-signalveiens transkripsjonelle hovedregulator [3][4]. På samme tid finnes det en rekke andre kreftcellelinjer der hemming av tankyrase fører til redusert vekst som er uavhengig av endret aktivitet i WNT/β-catenin-signalveien [4].

Med å finne en mer generell biomarkør som siktemål ble 660 kreftcellelinjer testet for deres cellevekstsensitivitet etter behandling med den nyoppdagede tankyrasehemmeren G007-LK. Blant kreftcellelinjene som utviste særskilt cellevekstsensitivitet ble fem cellelinjer valgt ut for videre analyse: ABC-1 fra ikke-småcellet lungekreft, OVCAR-4 fra eggstokkreft, A-498 fra nyrecellekreft og til slutt COLO320DM og SW480 fra tarmkreft.

En genutrykksanalyse påviste at genet ”B-cell lymphoma 2 modifying factor” (*BMF*) var kraftig oppregulert i den særdeles cellevekstsensitive cellelinjen ABC-1. Det kraftige uttrykket av *BMF* kunne ikke sammenføres med endret utrykk av *AXIN2* mRNA som uttrykkstyres av WNT/β-catenin-signalveiaktivitet [5].Videre ble det oppdaget at *BMF*-transkripsjonen også var oppregulert i cellelinjene COLO320DM, OVCAR-4 og SW480 etter både 24 og 72 timers behandling med 1 μM G007-LK (Fig. 3-2A). I A498 celler ble økt *BMF*-transkripsjon kun observert etter 24 timers behandling (Fig. 3-2A). Samtidig med den oppregulerte transkripsjonen av *BMF* ble det i tillegg observert nedregulert transkripsjon av *AXIN2* i cellelinjene COLO320DM, OVCAR-4 og SW480 (Fig. 3-2A). I samtlige analyserte kreftcellelinjer ble proteinutrykket av AXIN1 stabilisert etter behandling med G007-LK i 72 timer men på samme tid var det kun i SW480 og COLO320DM at det ble observert en tydelig reduksjon i β-cateninnivåer (Fig. 3-2B, 3-4B).

Aktivering av kinasen AMPK, Thr172-fosforylert AMPKα [7], har av andre blitt satt i sammenheng med forhøyet transkripsjon av *BMF* [6]. Vi kunne ikke påvise endret fosforylering av AMPKα i ABC-1-celler behandlet med G007-LK (Fig. 3-3B). Tilsvarende var ikke mengden totalt-AMPKα påvirket i COLO320DM mens nivået av fosforylert AMPKα (Thr172) var bemerkelsesverdig forhøyet etter 72 timers G007-LK-behandling (Fig. 3-4B, høyre). Satt i motsetning var nivåene av totalt-AMPKα redusert i tankyrasehemmede COLO320DM-celler behandlet med esiRNA mot *BMF* når sammenliknet med celler kun behandlet med siRNA mot *BMF*. Likevel ble økt fosforylering av AMPKα (Thr172) observert. Det kan konkluderes med at tankyrasehemming påvirker nivåene av AMPKα-protein kun ved fravær av *BMF* men at G007-LK øker fosforylering av AMPKα (Thr172) uavhengig av tilstedeværelse av *BMF* (Fig. 3-4B, høyre).

For å oppsummere: (i) *BMF*-transkripsjon videreføres i dette arbeidet som en potensielt mer generell indikativ biomarkør for tankyrasehemming i kreftceller sammenliknet med den tidligere benyttede biomarkøren β-catenin (Fig. 3-2A), (ii) vi påviser en regulatorisk interaksjon mellom *BMF* og AMPKα i COLO320DM som avhenger av tankyraseaktivitet (Fig. 3-4B, høyre) og (iii) vi legger for dagen at fosforylering av AMPK øker etter G007-LK-avhengig tankyrasehemming, kanskje også AXIN1 stabilisering, i COLO320DM (Fig. 3-4B, høyre).

# 1. Introduction

## 1.1 The WNT signaling pathways

In the 1980s, it was discovered that a retrovirus, the mouse mammary tumor virus, induced breast cancer in mice by causing activating mutations in the integration site *Int1* of mouse [8]. Later findings revealed that "*Int1*" was a homolog of the earlier discovered *Drosophila* segment polarity gene "*wingless"* [8]. Hereby, the name wingless-type mammary tumor virus integration site (WNT) was chosen for the *Int1*/*wingless* family [8]. Various WNT signaling pathways have been described including: i) The planar cell polarity pathway, ii) The WNT/$Ca^{2+}$ pathway, iii) The WNT-receptor-like tyrosine kinase pathway, iv) The WNT-receptor tyrosine kinase-like orphan receptor 2 pathway and v) The canonical WNT/β-catenin pathway [9][10][11]. Common to all these signaling pathways is that they get activated upon binding of the WNT ligands to the seven-pass transmembrane cell-surface receptor protein frizzled (FZD), and the co-receptor low density lipoprotein receptor-related protein 5/6 (LRP5/6) [12]. WNTs are glycoproteins with linked fatty acid chains at the N-terminus that enhances their binding affinity to the cell surface receptors [12]. Disheveled (DSH) is then recruited and activated for signal transduction downstream of the WNT/FZD/LRP complex and one of the WNT signaling pathway is triggered depending upon these signals [13].

## 1.1 The canonical WNT/β-catenin pathway

Among the WNT signaling pathway, the canonical WNT/β-catenin pathway (hereafter referred to as WNT pathway) is the most extensively studied pathway [12]. In the WNT pathway, β-catenin (the armadillo protein containing 12 armadillo repeats and 781 amino acids) plays a crucial role as a transcriptional modulator of WNT pathway target genes [5]. Expression of WNT pathway target genes are required in cell development and proliferation, and influence the differentiation and growth of embryonic cells, organs and regeneration of stem cells [5]. Proto-oncogenes like: V-myc avian myelocytomatosis viral oncogene homolog (*C-MYC),* jun proto-oncogene *(C-JUN),* cyclin D1(*CYCLIN-D1*), are a few of more than a 100 identified target genes of the WNT pathway [12].

**WNT pathway inactive state**

The WNT pathway is inactivated in the absence of WNT ligand [5]. The β-catenin destruction complex (DC) is active and cytoplasmic β-catenin is continuously degraded by the DC [5]. The DC consists of four main components: Axis inhibition protein 1 (AXIN1) or axis inhibition protein 2 (AXIN2)(AXIN1/2), casein kinase 1α (CK1α), glycogen synthase kinase 3β (GSK3β) and adenomatous polyposis coli (APC). The scaffolding protein, AXIN1/2, is the rate limiting element of DC assembly [5]. The priming kinase CK1α phosphorylates β-catenin at the N-terminus at serine (Ser)-45 which is followed by GSK3β phosphorylation at theronine (Thr)-41, Ser-37 and Ser-33. CK1α and GSK3β also phosphorylate the DC-scaffolding proteins AXIN1/2 and APC [14][12]. These events lead to the DC stabilization

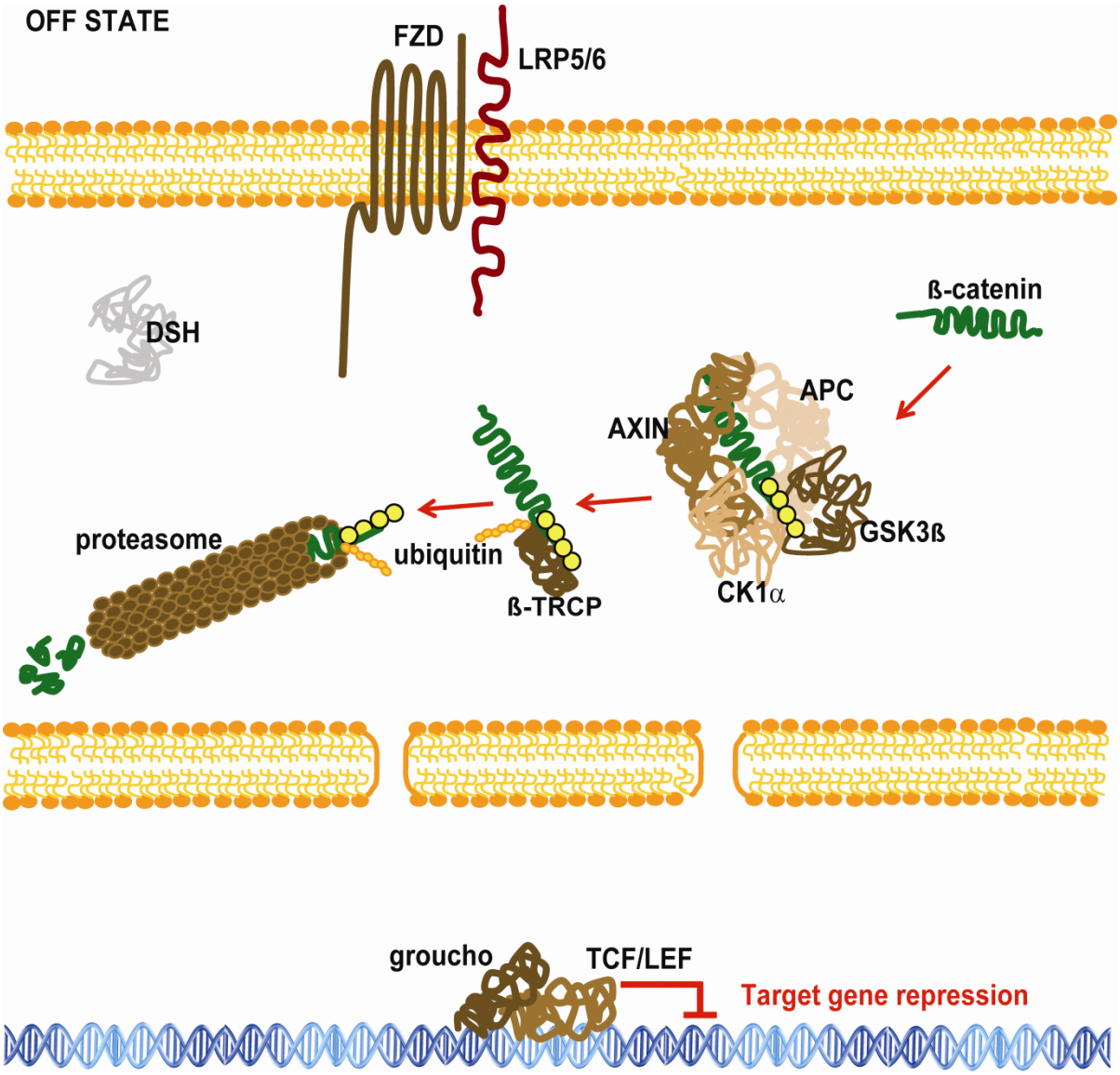


and β-catenin gets marked for ubiquitination. β-transducin-repeat-containing protein (β-TRCP), an E3 ligase, ubiquitinates cytoplasmic β-catenin which is subsequently degraded by the proteasome (Fig. 1-1)[12][15]. Cooperatively, these events inhibit translocation of the cytoplasmic β-catenin to the nucleus and WNT pathway target gene transcription is repressed by T-cell factor/lymphoid enhancer factor (TCF/LEF) and groucho complex [12].

**WNT pathway active state**

The WNT pathway is activated upon binding of WNT proteins to the cell-surface receptor protein FZD and the co-receptor LRP5/6 [12]. The WNT/FZD/LRP5/6 complex along with DSH attracts the components of the DC to the plasma membrane [16]. AXIN1/2 binds to the WNT/FZD/LRP signalosome [16][17]. CK1γ and GSK3β phosphorylate the tail of LRP in the PPPSPXS (P, proline; S, serine or theronine, X, a variable residue) motif [12][17]. Consequently, formation of the DC complex and the N-terminal phosphorylation of the β-catenin is inhibited. The non-phosphorylated active β-catenin (ABC) accumulates in the cytoplasm and is subsequently translocated to the nucleus. The nuclear β-catenin dislocates

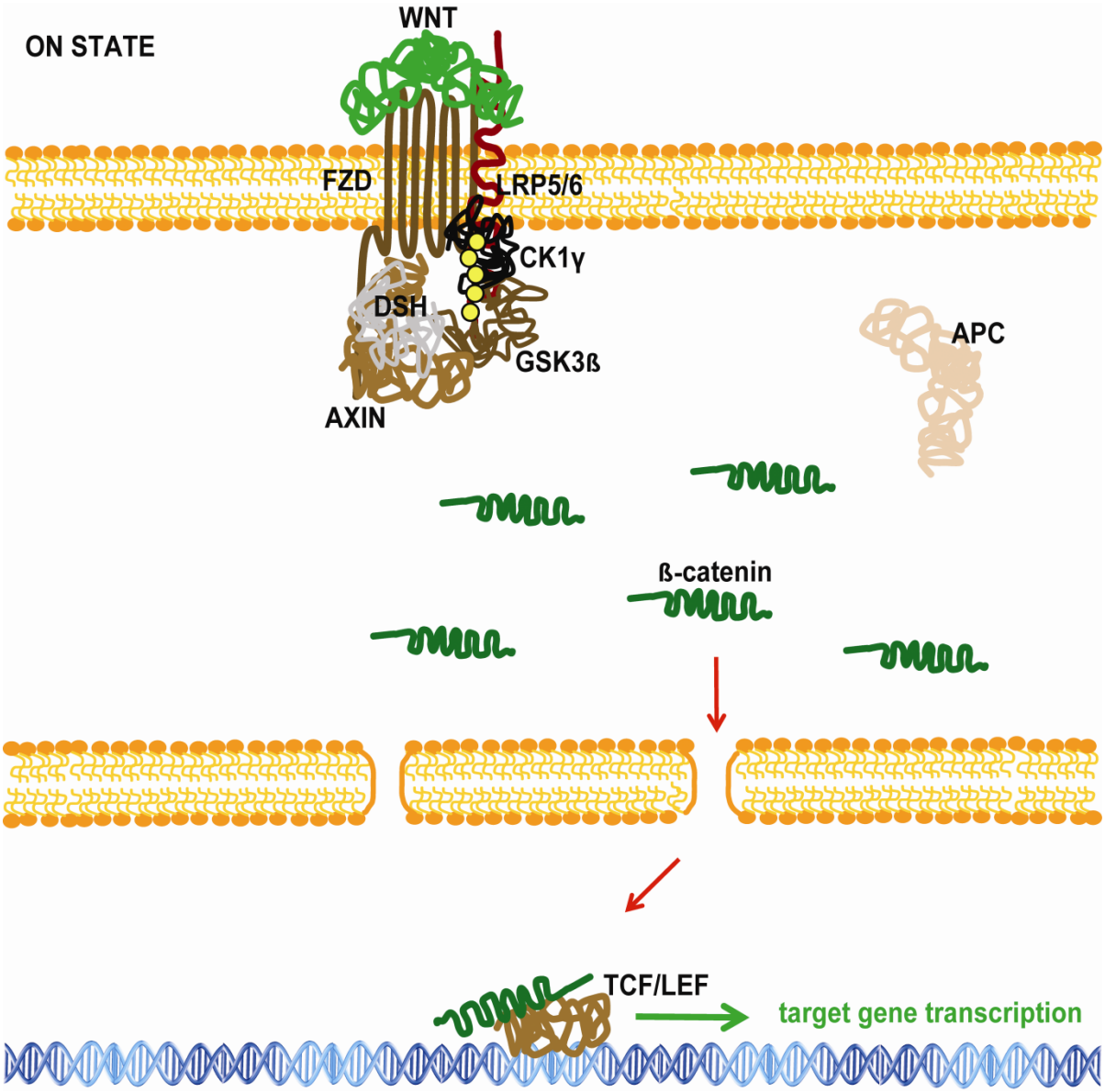


groucho (the repressor) and binds to the T-cell factor/lymphoid enhancer factor (TCF/LEF) gene regulatory proteins and mediates transcription of the WNT pathway target genes for example: *C-MYC, C-JUN, CYCLIN-D1* (Fig. 1-2)[12][15][18].

The WNT pathway maintains homeostasis by regulating expression of its components; AXIN2, TCF1, LEF1, naked (NKD), FZD, LRP and dickkopf-related protein 1 (DKK1), thus forming either a negative or positive feedback loop regulatory system [18]. Activated WNT pathway increases transcription of *AXIN2*, *DKK1* and *NKD* and decreases transcription of *FZD* and *LRP6*, thus forming a negative feedback loop that will reduce the activity of the WNT pathway [19][12]. Oppositely, transcription of R-spondin (*RSPO)* and *TCF/LEF* is induced upon enhanced activity of the WNT pathway, thus forming a positive feedback loop that will increase the activity of the WNT pathway [12].

## 1.2 WNT pathway in cancer and disease

Accumulating evidence suggests that malfunctioning of the WNT pathway or its components leads to the development of various diseases including cancer [20] . Activating mutations at

the N-terminal phosphorylation site of β-catenin and deactivating mutations in APC and AXIN are found in a large number of colon cancers. These mutations lead to elevated nuclear β-catenin levels [21][22]. Consequently, β-catenin/TCF/LEF dependent transcription is elevated [21]. Aberrant inhibition of the WNT pathway antagonists like secreted frizzled related proteins (SFRPs) [22], DKKs [23] and WNT inhibitory factors (WIFs) [24], and abnormal upregulation of the WNT pathway inducers like WNTS, FZD and DSH lead to the pathological and hyperactivated WNT pathway activity which is a major cause of various cancers [25][26].

The WNT pathway and its components are involved at several stages of the mitotic cell cycle [27]. The mitotic cell cycle is the process in which a somatic cell grows, synthesize DNA, duplicate chromosomes and eventually divide into the two identical daughter cells. The somatic cell growth cycle includes the following steps: i)The cell grows and genes are transcribed for the normal functioning cell in the gap 1 (G1) phase. ii) DNA replication and chromosome duplication into identical sister chromatids occurs in the synthesis (S) phase. iii) The cell grows and prepares for mitosis in the gap 2 (G2) phase. iv) Chromosome condensation and segregation takes place in the mitosis. v) Eventually, the parent cell divides into two identical daughter cells in the cytokinesis phase [28]. The cell cycle is controlled by the cyclin dependent kinases (CDK) at the check points to inhibit the cell cycle progression of any damaged cell. CDKs are regulated by the cyclins and cyclins repressors [29]. *C-MYC* is a direct WNT pathway target gene [30]. C-MYC upregulation due to enhanced activity of the WNT pathway leads to the elevated levels of cyclin D [31] and may simultaneously suppress the expression of the cyclin-D antagonists [32]. Toghether, these events lead to the rapid G1 phase and mediate tumor cell formation [33]. In addition, components of the WNT pathway, AXIN/GSK3/β-catenin are found at the centrosomes during microtubular growth and spindle construction [27]. Expression of AXIN/APC is elevated at the centrosomes during chromosome segregation in the mitosis [34][27][35]. LRP6 and intracellular β-catenin levels are heightened during the G2/mitosis phase [36][27]. In conclusion, the WNT pathway and its components work tightly with the mitotic cell cycle machinery [27], and therefore, abnormal WNT pathway activity may lead to the growth of cancer cells.

## 1.1 Tankyrase 1 and 2

Tankyrase 1 [telomeric repeat factor (TRF1)-interacting ankyrin-related adenosine diphosphate (ADP)-ribose polymerase; TNKS1/ARTD5/PARP5a] and tankyrase 2 (TNKS2/ARTD6/PARP5b)(TNKS1/2) are members of the Diphtheria toxin-like ADP-ribosyltransferase (ARTD) family [37]. This family consists of 17 different ARTDs, also referred to as poly(ADP-ribose) polymerases (PARPs)[38]. This highly conserved protein family is responsible for mono (ADP-ribose)sylation (MARsylation) and poly(ADP-ribose)sylation (PARsylation) of target proteins by their C-terminal catalytic ADP-ribosyltransferase (ART) domain, also called the PARP domain [38]. During MARsylation, only a single monomer of ADP-ribose is added to the target protein, while during

PARsylation, the poly(ADP)-ribose (PAR) chain is formed by adding new monomers of ADP-ribose, thus forming a PAR chain [38].

TNKS1/2 belong to the subgroup that PARsylates target proteins [37]. TNKS1/2 full length structure are not yet obtained but TNKS1 catalytic ART domain is fully characterized (Fig. 1-3)[39][40]. The catalytic ART domain possesses an acceptor site for binding to the target protein and a donor site for binding and hydrolysis of nicotinamide adenine dinucleotide ($NAD^+$)[39][41]. The donor site is further divided into two sub-sites: The nicotinamide (NI) binding site and the adenosine (AD) sub-site [39][42]. TNKS1/2 share 86% sequence identity in the catalytic ART domain [40] and are also functionally equal [1].

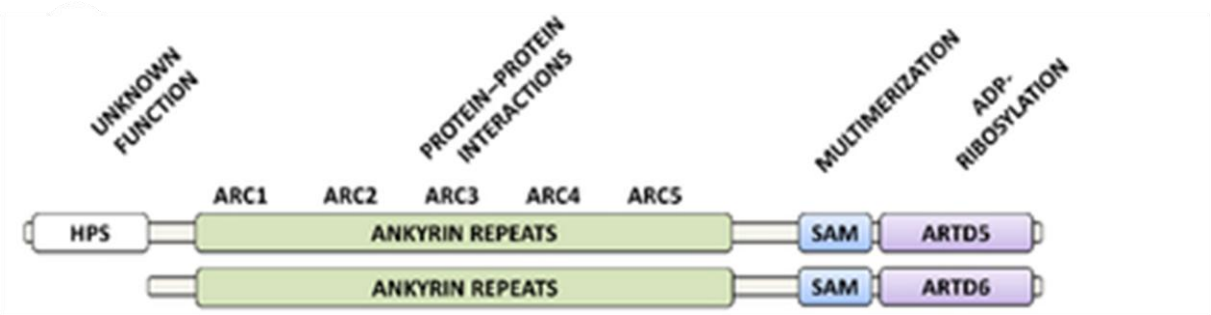


**Figure 1-3:** The domains of TNKS1 (ARTD5) and TNKS2 (ARTD6). The catalytic ARTD domain is responsible for ADP-ribosylation, the SAM domain for multimerization and the ankyrin repeats for protein-protein interaction. The function of the HPS domain is unknown [1].

During the PARsylation process, $NAD^+$ is used as a substrate and cleaved into ADP-ribose and nicotinamide by the catalytic domain. The ADP-ribose monomer is transferred to lysine or glutamate residues in the target protein, while nicotinamide is released from the catalytic site in the initiation reaction. Elongation can then occur by addition of new monomers of ADP-ribose to the existing modification and thus forming a PAR chain [37][38][1](Fig. 1-4).

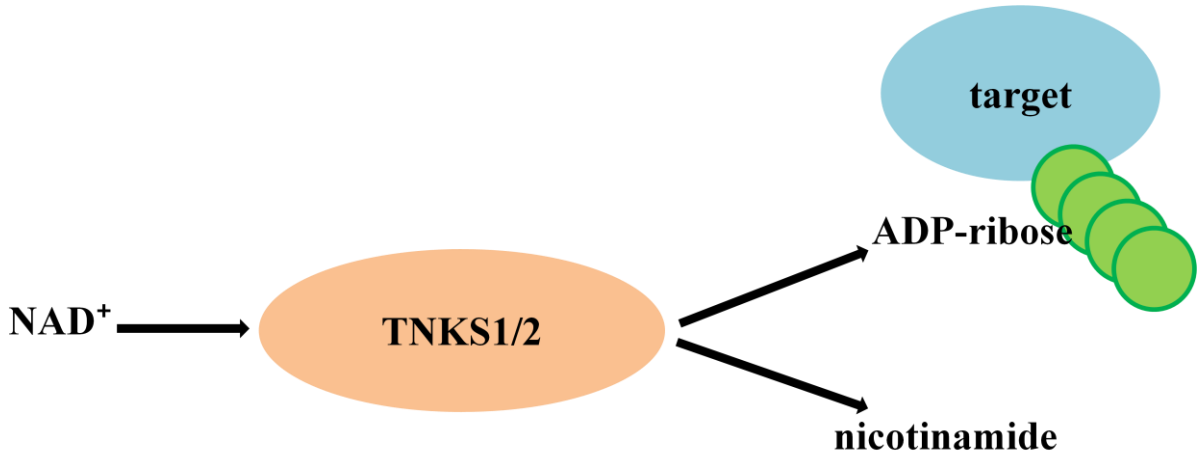


**Figure 1-4:** During PARsylation, TNKS1/2 uses $NAD^+$ as a substrate and cleaves it into ADP-ribose and nicotinamide. Nicotinamide is released while ADP-ribose monomers are added to the target protein forming a PAR chain.

Unlike other PARPs, TNKS1/2, in addition to the catalytic ART domain, also contains a sterile alpha motif (SAM) domain and an ankyrin repeat domain. The SAM domain functions in multimerization and the ankyrin repeat domain functions in protein-protein interactions. The ankyrin repeat domain can be divided into five different ankyrin repeat clusters (ARC)(Fig. 1-3)[1][43][42]. Four of these five ARCs: ARC1, ARC2, ARC4 and ARC5, have consensus tankyrase binding motifs (TBM) with the general sequence RXXPXGXX. These TBMs can next connect the RXXPXGXX domains in interacting target proteins to the ARC [2]. TNKS1 also possesses a functionally unknown histidine, proline and serine (HPS)-rich domain [1][43](Fig. 1-3). In addition to PARsylation of target proteins, TNKS1/2 can also undergo auto-PARsylation [1]. Oppositely, PAR-chains conjugated to the targets can be removed by poly(ADP-ribose) glycohydrolase (PARG)[44].

## 1.3 Cellular mechanisms orchestrated by tankyrase

TNKS1/2 along with its binding partners plays a crucial role in a number of cellular functions: The WNT pathway, telomere maintenance, mitosis and glucose metabolism.

**Tankyrase regulates AXIN1/2 degradation and the WNT pathway activity**

AXIN1/2 is one of the binding partners of TNKS1/2 [42]. In humans, two types of AXIN proteins are found: AXIN1 has 826 amino acids and AXIN2 has 840 amino acids [42]. The link between TNKS1/2 and AXIN1/2 with respect to the WNT pathway came first to light in 2009 [3]. A WNT-responsive Super-Topflash luciferase (ST-LUC)-based high-throughput screening in HEK293-cells identified XAV939 as a WNT pathway inhibitor. It was found that XAV939 causes β-catenin degradation through promoting AXIN1/2 protein stabilization. Expression levels of both AXIN1/2 proteins are increased upon TNKS inhibition by XAV939 [3]. Later independent studies revealed several TNKS1/2 inhibitors : WIKI-4 [45], G244-LM [4], PJ34 [46], JW55[47], JW74 [48] and G007-LK [4]. XAV939 [3] , G244-LM [4] and PJ34 [46] inhibit TNKS1/2 and PARP-1 by binding to the NI sub-site in the ART domain. IWR-1 [49], JW55 [47], JW74 [48], and G007-LK [4] specifically inhibit TNKS1/2 by binding to the AD sub-site of TNKS1/2 in the ART domain.

AXIN1/2 proteins are negative regulators of the WNT pathway [3][5]. As mentioned earlier, AXIN1/2 proteins promote β-catenin destabilization through the DC, and thus, inhibit the WNT pathway [3][5]. *AXIN1* is constitutively transcribed but *AXIN2* is a WNT pathway target gene. *AXIN2* transcription is induced upon increased WNT pathway signaling through the β-catenin *TCF/LEF* complex in the nucleus, forming a negative feedback loop for WNT pathway regulation [5].

AXIN1/2 may be PARsylated by TNKS1/2. TNKS1/2 adds PAR-chain to the AXIN1/2 that marks it for ubiquitination by ring finger protein 146 (RNF146), an E3 ligase, which is followed by its degradation in the 26S proteasome [42](Fig. 1-5). Since AXIN1/2 is the main rate limiting element of the DC, AXIN1/2 degradation leads to destabilization of DC which

subsequently leads to an increase of the WNT pathway signaling even in the absence of a WNT ligand [42].

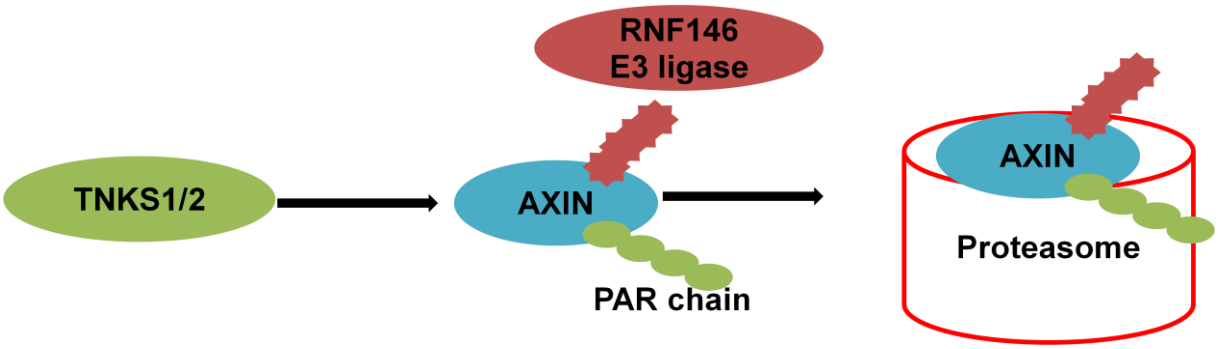


**Figure 1-5**: A scheme representing that TNKS mediated PARsylation signals RNF146 to ubiquitinate AXIN1/2. Ubiquitination of AXIN1/2 leads to its proteasomal degradation.

### Tankyrase in glucose metabolism

TNKS1/2 and AXIN also play roles in the sub-cellular translocation of glucose transporter type 4 (GLUT4)[1]. The insulin sensitive GLUT4 regulates glucose uptake in the muscle and fat cells [50]. Upon insulin stimulation, insulin responsive aminopeptidase interleukin 1 receptor antagonist (IRAP) along with TNKS1/2, AXIN and kinesin family member 3A (KIR3A) complex mediate GLUT4 translocation from the golgi apparatus to the cell surface [51][50]. Mice deficient of TNKS-1 develop glucose metabolism disorders and exhibit decreased adiposity [52].

### Tankyrase in telomere maintenance

TRF1 binds to the tandem repeat sequences of the telomere and induces folding of the chromatin structure so that the ends of the chromosomes are not accessible for replication by telomerase [53]. TNKS1 PARsylates TRF1 which leads to TRF1 proteosomal degradation. In this way TRF1 proteins are untied and the chromatin structure opens up. The telomeric repeat sequence is now available for telomerase and can be elongated. Thus, TNKS1 may maintain telomere length in tumors by PARsylating TRF1 [1]. It is important to note that telomerase is not active in normal adult somatic cells but only in embryonic cells, reproductive cells and stem cells [53]. A part of the telomere is lost upon each cell replication cycle in somatic cells [53]. However, in some tumors the telomere length can be maintained and is linked to PARsylation and degradation of TFR1 via TNKS1 [2].

### Tankyrase in mitosis

TNKS1 along with its target nuclear mitotic apparatus protein (NuMA) is involved in sister chromatids telomere cohesion [43]. During mitosis, TNKS1 and NuMA are required for spindle poles formation [1]. Upon TNKS1 knock down, the cells formed defected mitotic

spindle poles and were constantly attached at the telomeres. The exact mechanism of action is still ill-defined [43].

TNKS role in aberrant WNT pathway activity, telomere homeostasis in cancer cells, spindle formation in mitosis, and glucose metabolism regulation makes TNKS1/2 inhibitors potent drug target against various diseases and cancer.

## 1.2 Discovery of the WNT pathway and tankyrase inhibitor: G007-LK

JW74 was identified as a small molecule inhibitor of the WNT pathway from a high-throughput screen using a WNT-responsive Super-Topflash destabilized enhanced green fluorescent protein (ST-d1EGFP) reporter assay in HEK293 cells [48]. JW74 reduced WNT pathway signaling in HEK293 cells with half maximal inhibitory concentration ($IC_{50}$) value of 790 nmol/L but had no inhibitory effects on the sonic hedgehog signaling pathway or the nuclear factor kappa-light-chain-enhancer of activated B cells (NF-κB) pathway [48]. JW74 *in vivo* efficacy was tested in the *Xenopus laevis* axis duplication assay. In this assay, *xwnt8* mRNA is injected into the ventral blastomeres of the *Xenopus laevis* embryo which induces double axis formation. Upon treatment with WNT pathway inhibitory molecules, double axis formation can be reduced. JW74 inhibited double axis formation in *Xenopus laevis* embryos up to 87% and led to the conclusion that JW74 is a WNT pathway inhibitor [48]. JW74 has also been tested in $Apc^{Min}$ (multiple intestinal neoplasia, Min) mice [54]. The $Apc^{Min}$ mice have genetically engineered mutations in one allele of *Apc* [54]. *Apc* mutations are a general cause of colorectal cancer [55]. Therefore, these $Apc^{Min}$ mice are prone to develop colorectal cancer [54] and provide an ideal model to test drugs against colorectal cancer. JW74 considerably reduced polyp-formation and polyp-enlargement in the colon and small intestine of $Apc^{Min}$ mice with a dosage of 150 mg/kg [48]. The mechanism of JW74 mediated WNT pathway inhibition was explored in a number of assays leading to the conclusion that JW74 inhibits WNT pathway at the GSK3β/AXIN/APC level of the DC [48].

JW74 also inhibits TNKS1/2 and reduces cell growth in osteosarcoma (OC) cell lines: KPD, U2OS, and SaOS-2 [56]. WNT pathway is also inhibited and caspase-3-dependent apoptosis is induced in U2OS upon JW74 treatment [56]. JW74 exposure promotes cell differentiation in U2OS and SaOS-2 [56].

To improve JW74 metabolic stability, structural-activity relationship (SAR) assays were conducted. 1-2-4 triazole core was found to be essential for JW74 activity [57]. The compound, JW74, was modified beholding the 1-2-4 triazole core (Fig. 1-6)[57]. 4-{5-[(E)-2-{4-(2-chlorophenyl)-5-[5-(methylsulfonyl)pyridin-2-yl]-4H-1,2,4-triazol-3yl}ethenyl]-1,3,4-oxadiazol-2-yl}benzonitrile (G007-LK) is an analogue of JW74 (Fig. 1-6)[57] which is metabolically stabilized against liver enzymatic degradation through SAR [57]. G007-LK is TNKS1/2 specific with the $IC_{50}$ values of 46 nM for TNKS1 and 25 nM for TNKS2, and a cellular $IC_{50}$ value of 50 nM [57]. It is a small molecule with a molecular weight of 529.96 Da

and binds to the histidine 1048 of the adenosine pocket of TNKS1/2 and effectively inhibits TNKS1/2 from PARSylating its targets [57]. Since G007-LK does not bind to any other members of the PARP family, it is the most selective inhibitor of TNKS1/2 at present [57]. G007-LK has been proven to successfully decrease WNT pathway activity through TNKS1/2 inhibition in the following APC mutant colorectal cancer (CRC) cell lines: COLO320DM, SW403, HCT-15, DLD-1, LS-1034 and SW1417 [4]. Upon TNKS inhibition, AXIN levels are elevated and WNT pathway target gene expression is inhibited. Interestingly, TNKS inhibition in the CRC cell line HT29 leads to activation of the WNT pathway target gene expression [4].

G007-LK inhibits colony formation of COLO320DM and SW403 CRC cell lines *in vitro,* and reduces tumor formation and expansion in the xenografts models of COLO320DM and SW403 [4].

Thus, it can be concluded that G007-LK is a TNKS1/2 inhibitor that substantially reduces WNT pathway activity [4][57]. G007-LK inhibits WNT pathway by stabilizing AXIN through TNKS1/2 inhibition and affects proliferation in a number of cancer cell lines [4]. G007-LK sensitive cancer cell lines display TNKS1/2 inhibition upon G007-LK treatment and exhibit either one, both or none: i) Altered proliferation upon TNKS1/2 inhibition. ii) WNT pathway inhibition upon TNKS1/2 inhibition [4]. G007-LK's target specificity, efficacy and metabolic stability make it a potential therapeutic drug candidate against WNT pathway dependent cancer [4][57].

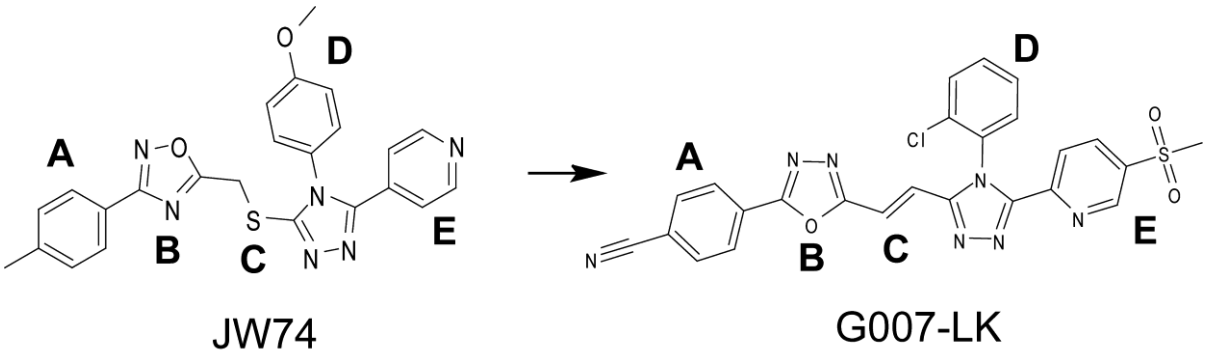


**Figure 1-6:** A scheme representing modifications in the regions A,B,C,D and E in JW74 to establish its 1-2-4 triazole based analouge G007-LK [57].

## 1.3 BCL-2 superfamily and BMF

The B-cell lymphoma 2 (BCL2) superfamily is the main regulator of programmed cell death. It consists of a number of regulatory proteins that can induce or repress caspase-dependent and independent cell death [58]. BCL-2, BCL-extra large (BCL-XL), BCL2-like-protein-2 (BCL-W), Myeloid cell leukemia 1 (MCL-1) and BCL2-related protein (A1), are classified as the anti-apoptotic proteins of the BCL2 family that express all the four structural BCL-2 homology (BH) domains of the family, and antagonize apoptosis [59]. The pro-apoptotic

proteins fall into the two categories: The killers, BCL2-like protein 4 (BAX) and BCL2-antagonist/killer 1 (BAK), that share multi-domain: BH1, BH2 and BH3 homology, and the BH3-only proteins. The BH3-only proteins can be further divided into two groups: i) Activators that directly interact with killers, ii) Sensitizers that bind to the anti-apoptotic proteins so that activators can be released to trigger the killers and eventually lead to apoptosis [59].

B-cell lymphoma 2 modifying factor (BMF) falls into the category of BH3-only, sensitizer and pro-apoptotic proteins [59]. The *BMF* gene is located on the chromosome 15q14 in humans [60]. Various isoforms of the protein BMF exist due to mRNA alternative splicing [60]. Under physiological conditions in the cells, BMF is segregated to the myosin V motor complex through its interaction with the dynein light chain 2 (DLC2) in the cytoskeleton [61]. Certain stress conditions, such as UV radiation, detachment of adherent cells from the extracellular matrix or exposure to actin depolymerization drugs, release BMF to the mitochondria [61]. BMF is released from the V motor complex along with the DLC2 when triggered by anoikis [61]. In the mitochondria, BMF may bind to the pro-apoptotic protein A1 (Fig. 1-7)[62] to promote mitochondrial cytoplasmic membrane permeabilization which eventually leads to apoptosis [59].

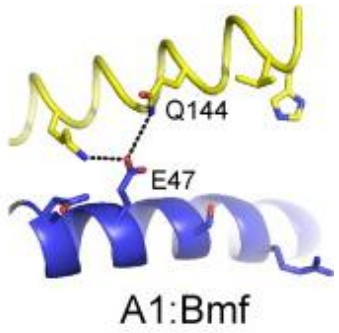


**Figure 1-7:** The BH3 domain (yellow) of the pro-apoptotic protein, BMF, interacts with the α2-domain (blue) of the anti-apoptotic protein, A1 [62].

BMF upregulation has been observed through the following pathways: i) Transforming growth factor beta (TGFβ)-mediated signals [63], ii) Histone deacetylase inhibitor (HDACi) treatment [64], iii) C-JUN NH(2)-terminal kinase (JNK) phosphorylation [65], iv) Cell stressors that repress CAP-dependent protein synthesis [66] and v) Adenosine monophosphate-activated protein kinase (AMPK) activation [6][67].

i) Transforming growth factor beta (TGFβ)-mediated signals upregulate *BMF* gene expression through the mothers against decapentaplegic homolog (SMAD4) or mitogen-activated protein kinase (p38) that leads to apoptosis [63].

ii) Histone deacetylase inhibitor (HDACi) treatment with FK228 hyperacetyltes histone 3 and 4 at the promoter domain of the *BMF* gene resulting in *BMF* transcription upregulation and mitochondrial pathway apoptosis in the oral and esophageal squamous cancer cells [64].

iii) Bortezomib (PS341) is a pharmacological inhibitor of 26S proteasome and causes apoptosis in a broad range of cancers [65]. Upon investigation, it was found that PS341 leads to JNK and BMF dependent apoptosis in the A172 and T98G cells. PS341 exposure activates JNK [65] and activated JNK phosphorylates BMF in the DLC2 binding motif region (DKATQTLSP)[68]. This phosphorylation of BMF by JNK causes BMF release from the V motor complex and BMF is localized to mitochondria to initiate apoptosis [65][68].

iv) Inactivating mutations in the hepatocyte nuclear factor $_1$A (*HNF$_1$A)* gene cause excessive apoptosis of the beta (β)-cells which disrupts glucose metabolism and causes maturity-onset diabetes-of-the-young type 3(MODY3)[69]. To study the function of *HNF$_1$A* gene, the rat insulin secreting β-cell derived line, INS-1, was stably transfected with overexpressing wild-type *HNF$_1$A* (*WT-HNF1A*) or dominant-negative sm6 mutant of *HNF$_1$A* (DN-HNF1A) plasmids [69]. The publication demonstrated that excessive expression of DN-HNF1A leads to the following: 1) *Glut4* mRNA and ATP levels decrement. 2) Adenosine monophosphate (AMP)-activated protein kinase (AMPK) activation and 3) *Bmf* mRNA upregulation and apoptosis. Gene knock down of AMPK or chemical inhibition of AMPK with compound C decreased *Bmf* levels, while activation of AMPK with AICAR increased *Bmf* levels. Therefore, the study concluded that *Bmf* is upregulated upon AMPK activation to cause apoptosis in INS-1 cells [6].

Apart from being a pro-apoptotic protein in the hematopoietic system [61][64][66][70][6], BMF also plays an anti-apoptotic role [67]. It was found that *Bmf* protects neuronal cell death caused by prolonged seizures (SE) in the mouse hippocampus [67]. SE causes ATP depletion in the brain cells and thus activates AMPK. Activated AMPK was found to upregulate *Bmf* transcription and protect against neuronal cell death. Pharmacological inhibition of AMPK through compound C resulted in decreased levels of *Bmf* transcripts and increased cell death. Mice deficient for *Bmf* gene were found to be more prone to SE mediated cell death [67].

## 1.4 Role of AXIN in AMPK activation

Apart from being the key regulator of cell metabolism [7], adenosine monophosphate (AMP)-activated protein kinase (AMPK) is also involved in cell polarity and cell growth maintenance [71]. AMPK maintains homeostasis in cell metabolism by switching between catabolism and anabolism, depending on the AMP/Adenosine triphosphate (ATP) ratios [7]. AMPK is a heterodimer that consists of the α-catalytic subunit, β and γ-regulatory subunits. The subunits of AMPK also exist in different isoforms like α1, α2, β1, β2, γ1, γ2 and γ3. AMPK is activated upon phosphorylation of theronine (Thr)-172 at the α-catalytic subunit by the kinase complex: Liver kinase B1(LKB1)-STE20-related kinase adapter protein (STRAD)-mouse protein 25 (MO25)[7]. LKB1 is the primary kinase, while the STRAD and MO25 are accessory subunits of the kinase complex. In a low energy state, AMP/ATP ratio is increased. AMP binds to the γ-regulatory subunit, causing a conformational change in the heterodimer AMPK such that Thr172 phosphorylation is enhanced, and dephosphorylation by the phosphatase C2α is inhibited [7].

Mechanism of AXIN driven AMPK activation was investigated by Zhang.et.al [72]. It was found that AXIN knock down in the mouse liver reduced AMPK phosphorylation and increased hepatic triglyceride. Similar results were found in vitro studies of the human liver cells L02, the hepatic cancer HEpG2 cells and MEF cells. To explore the mechanism of AXIN mediated AMPK phosphorylation, a number of immunoprecipitation assays were carried out. It was discovered that AMPK, LKB1, STRAD, MO25 precipitate with AXIN. STRAD and MO25 immunoprecipitation with AXIN was found to be LKB1-dependent and AXIN knock down impaired LKB1-STRAD-MO25 interaction. Domain mapping revealed that AXIN residues at amino acid 507-731 were crucial to binding LKB1 and AMPK. And AXIN mediates AMPK phosphorylation through the LKB1 kinase. Further analysis revealed that in the low energy state, AMP binds to the AMPK and boosts AXIN and myristoylated AMPK binding. AXIN accommodates AMPK and LKB1 forming a AMPK-AXIN-LKB1 complex and mediates AMPK phosphorylation at the α-subunit site Thr172 through LKB1 (Fig. 1-8)[72].

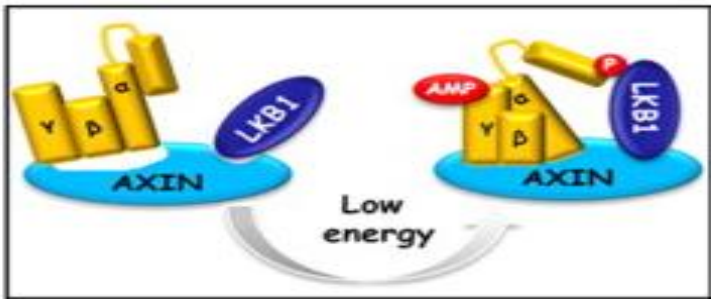


**Figure 1-8:** A possible mechanism of AXIN mediated AMPK activation. AMP enhances AMPK binding to AXIN. AXIN at the amino acid region 507-731, accommodates AMPK and LKB1 forming a AMPK-AXIN-LKB1 complex and mediates AMPK phosphorylation at the α-catalytic subunit site Thr172 through LKB1 [72].

## 1.5 Analysis of biomarkers in response to G007-LK treatment in the cancer cell lines

Deregulated WNT pathway activity plays a key role in a variety of cancers [5]. G007-LK inhibits WNT pathway by stabilizing AXIN through TNKS1/2 inhibition and affects proliferation in a number of cancer cell lines [4]. G007-LK sensitive cancer cell lines display TNKS1/2 inhibition upon G007-LK treatment and exhibit either one, both or none: i) Altered proliferation upon TNKS1/2 inhibition. ii) WNT pathway inhibition upon TNKS1/2 inhibition [4].

To identify G007-LK sensitive cancer cell lines on a large scale, Genentech screened 600 different cancer cell lines. Additionally, NCI-60 human tumor cell panel was screened for sensitivity to the G007-LK through the drug development program (DTP) at the National cancer institute (NCI). G007-LK has also been tested by Lau et al. in a broad number of colon cancer cell lines [4]. Among the cancer cell lines that exhibited growth alteration in response

to G007-LK treatment, a few were chosen for analysis in this thesis which are mentioned as follows: i) ABC-1 non-small-cell lung cancer cell line from Genentech, ii) OVCAR-4 ovarian cancer cell line and A-498 renal cancer cell line from NCI-60 DTP, iii) COLO320DM CRC cell line tested by Lau.et.al [4]. Since SW480 CRC cell line exhibited growth inhibition upon JW74 (a G007-LK analogue)[48], it was also chosen for analysis.

*BMF* transcripts were strongly upregulated upon a qRT-PCR analysis conducted by Genentech in ABC-1 (Fig. 1-9) and COLO320DM. This upregulation was not accompanied with *AXIN2* mRNA decrease in ABC-1 (Fig. 1-9). Identification of biomarkers is a key step towards defining patient inclusion and exclusion criteria for the use of G007-LK as a medicine. Based on the results from Genentech's study, *BMF* was considered to be a potential biomarker for G007-LK sensitive cancer cell lines.

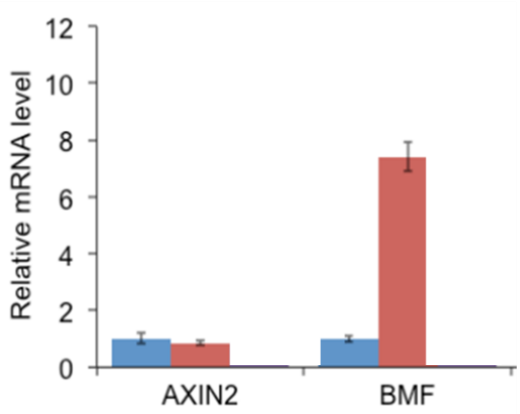


**Figure 1-9:** A qRT-PCR analysis from Genentech in ABC-1 cell line. Blue columns represent control and red columns represent relative target gene expression. Left, *AXIN2* transcripts are not considerably affected upon G007-LK treatment in the ABC-1 cell line. Right, *BMF* transcripts are strongly upregulated upon G007-LK treatment in the ABC-1 cell line.

The project aimed to validate if the cancer cell lines ABC-1, OVCAR-4, A498, COLO320DM and SW480 are G007-LK-sensitive. G007-LK-sensitive cell lines may display at least one of the following features: i) TNKS1/2 inhibition (usually observed as differently expressed TNKS1/2 protein levels), ii) Increased AXIN protein levels, iii) Decreased WNT pathway signaling and iv) Reduced proliferation [4]. Furthermore, the aim was also to explore BMF as a potential biomarker in response to G007-LK treatment, and investigate a potential interplay between AXIN, AMPK and BMF.

The AMPK-activation pathway was chosen to explore a potential interplay between AXIN1, AMPK and BMF upon treatment with G007-LK, because we found strong potential links between AXIN, AMPK activation and BMF in literature which are as follows: i) Recent studies claim that TNKS1/2 inhibition upon G007-LK treatment stabilizes AXIN protein levels [4]. ii) AXIN plays a crucial role in the assembly of AMPK activation complex and facilitates LKB1-mediated AMPK activation [72]. iii) Activated AMPK leads to *BMF* up regulation to cause apoptosis [6]. Taken together this data, we hypothesized that G007-LK stabilizes AXIN upon TNKS1/2 inhibition. AXIN stability enhances formation of AMPK activation complex LKB1-AXIN-AMPK, and mediates AMPK activation. Activated AMPK causes upregulation of *BMF* transcription (Fig. 1-10).

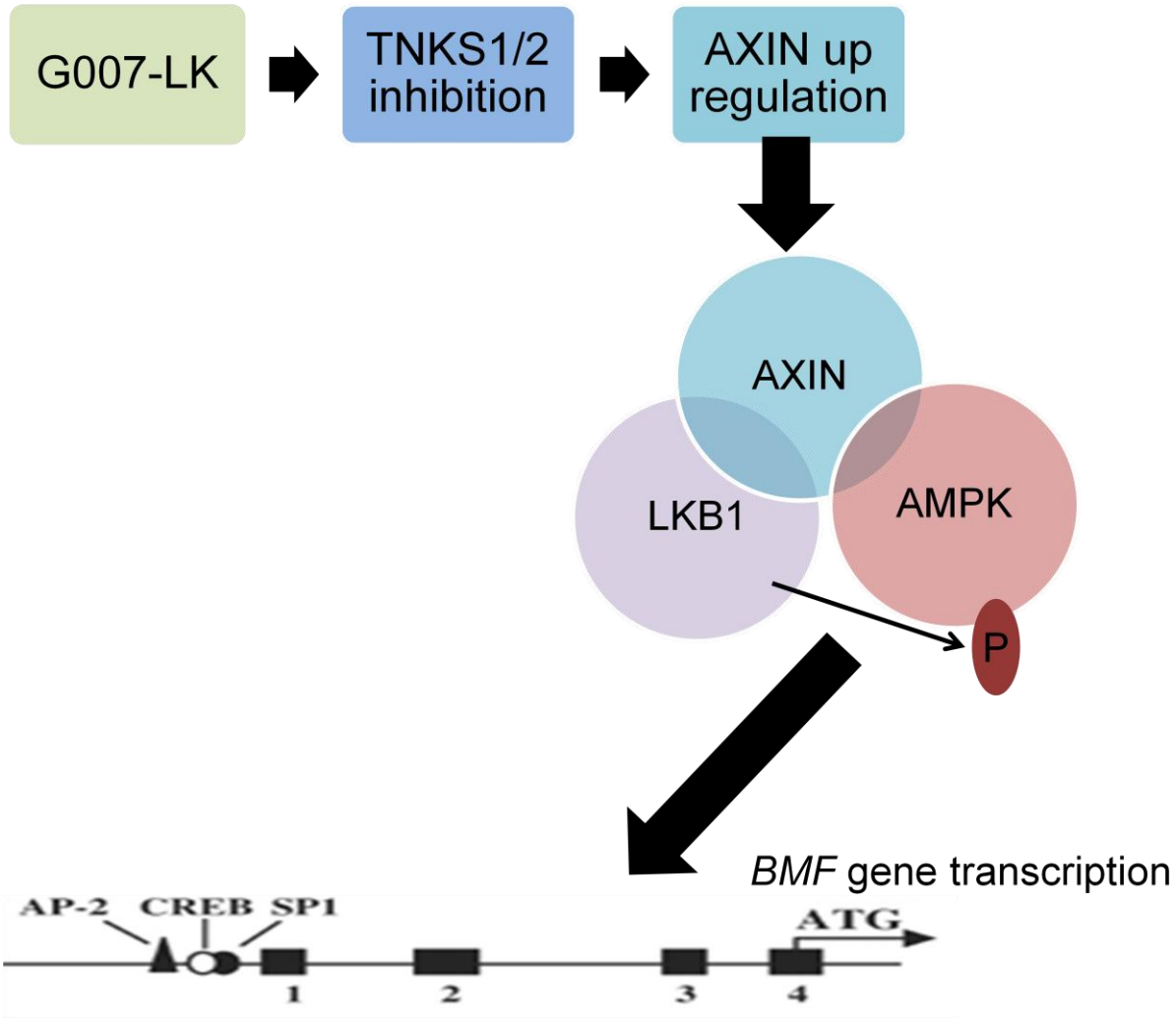


**Figure 1-10**: A scheme presenting a potential interplay of AXIN, AMPK and BMF upon G007-LK treatment. G007-LK inhibits TNKS1/2 from PARsylating AXIN. AXIN is stabilized and mediates AMPK phosphorylation through LKB1. Phosphorylated active AMPK upregulates *BMF*. The *BMF* gene with its promoter region is shown with promoter-specific transcription factor (SP1), adenosine 3',5'-monophosphate (cAMP) response element-binding protein (CREB) and activator protein (AP-2) are shown [64].

## 1.4 Aim of the study

The project aimed to validate if the cancer cell lines ABC-1, OVCAR-4, A498, COLO320DM and SW480 are G007-LK-sensitive. G007-LK-sensitive cell lines may display at least one of the following features: i) TNKS1/2 inhibition (usually observed as differently expressed TNKS1/2 protein levels), ii) increased AXIN protein levels, iii) decreased WNT pathway signaling and iv) reduced proliferation [4]. Furthermore, the aim was also to explore BMF as a potential biomarker in response to G007-LK treatment, and investigate a potential interplay between AXIN, AMPK and BMF.

# 2. Methods

## 2.1 Cell treatments and cell work

### 1.6 2.1.1 Cell culture

The adherent cancer cell lines ABC-1, A-498, COLO320-DM, HT29, OVCAR-4 and SW480 were cultured and maintained according to the supplier's recommendations (Table 2-1).

**Table 2-1:** Cell culture conditions for the respective cell lines used in this thesis.

| **Cell line** | **Species** | **Tissue** | **Medium*** | **Carbon dioxide ($CO_2$) in the incubator** | **Split ratio** | **Supplier*** | **Catalog number** |
|---|---|---|---|---|---|---|---|
| ABC-1 | human | lung | EMEM, 10% FBS, 5% P/S | 5% | 1:3 | JCRB | JCRB0815 |
| A-498 | human | renal | EMEM, 10% FBS, 5% P/S | 5% | 1:3 | NCI | ------ |
| COLO320-DM | human | colon | RPMI-1640, 10% FBS, 5% P/S | 5% | 1:3 | ATCC | CCL-220™ |
| OVCAR-4 | human | ovarian | RPMI-1640, 10% FBS, 5% P/S | 5% | 1:3 | NCI | ------- |
| SW480 | human | colon | L-15, 10% FBS, 5% P/S | Atmospheric $CO_2$ concentration | 1:3 | ATCC | CCL-228™ |

*EMEM: Eagle's minimum essential medium; FBS: fetal bovine serum; P/S: penicillin/streptomycin; L-15: Leibovitz's L-15 medium; JCRB: Japanese collection of research bioresources cell bank; ATCC: American type culture collection; NCI: National cancer institute.

The cells were inspected with a microscope on daily basis. Exponentially growing cells were sub-cultured up to maximum 20 passages. The general procedure followed for cell thawing, seeding, expansion and splitting is mentioned as follows.

**Thawing of cryo preserved cells**

1. Frozen cells were thawed in a water bath at 37 ˚C.
2. Resuspended thawed cells with 1 ml cell culture medium.
3. Transferred the cells to a 15 ml tube containing circa 8 ml cell culture medium and centrifuged for about 3 minutes (min) at 2000 rpm.
4. Discarded supernatant.
5. Resuspended the cells in the cell culture medium and transferred to the 25 $cm^2$ flask.

**Expanding of adherent cells**

1. Discarded the cell culture medium upon 70-80% confluence from the 25 $cm^2$ flask.
2. Washed with circa 5 ml phosphate buffered saline (PBS) to remove all cell culture medium.
3. Discarded all PBS.
4. Added 3 ml trypsin to detach the cells.
5. Incubated the cell culture flask at 37 ˚C for about 5 min (until the cells detach from the flask).
6. Resuspended cells in the flask using 5 ml pipette to remove cell clumps.
7. Transferred the cells into a bigger flask (From 25 $cm^2$ flask to 75 $cm^2$ flask and from 75 $cm^2$ flask to 175 $cm^2$ flask).

**Splitting of cells**

1. Discarded cell culture medium from the 70-80% confluent 175 $cm^2$ flask.
2. Washed with circa 5 ml PBS to remove all cell culture medium.
3. Discarded all PBS
4. Added 5 ml trypsin to detach the cells.
5. Incubated the flask at 37 ˚C for about 5 min.
6. Resuspended cells using 5 ml pipette to remove cell clumps.
7. Kept the required ratio of cells and discarded rest of the cells.
8. Added cell culture medium and placed it in the incubator at 37 ˚C.

**Cell seeding in a culture plate**

1. Counted number of cells with an automated cell counter TC 20 (BioRad).
2. Seeded the required number of cells in the 6 well plate (wp) for Western blot analysis and 12 wp for quantitative real time polymerase chain reaction (qRT-PCR) analysis (Table 2-2 and Table 2-3).

**Table 2-2:** Cell seeding densities and amount of cell culture medium used prior to treatment for respective cell lines.

| **Cell lines** | **Seeding density/well in a 6-wp for 24 h treatment (number of cells)** | **Seeding density/well in a 6-wp for 72 h treatment (number of cells)** | **Cell culture medium for 6-wp (ml)** | **Seeding density/well in a 12-wp for 24 h treatment (number of cells)** | **Seeding density/well in a 12-wp for 72 h treatment (number of cells)** | **Cell culture medium for 12-wp (ml)** |
|---|---|---|---|---|---|---|
| ABC-1 | $0.65 \times 10^6$ | $0.40 \times 10^6$ | 4 | $0.30 \times 10^6$ | $0.20 \times 10^6$ | 2 |
| COLO320DM | $0.65 \times 10^6$ | $0.50 \times 10^6$ | 4 | $0.30 \times 10^6$ | $0.20 \times 10^6$ | 2 |
| SW480 | $0.65 \times 10^6$ | $0.52 \times 10^6$ | 4 | $0.30 \times 10^6$ | $0.20 \times 10^6$ | 2 |
| A-498 | $0.65 \times 10^6$ | $0.40 \times 10^6$ | 4 | $0.30 \times 10^6$ | $0.20 \times 10^6$ | 2 |
| OVCAR-4 | $0.65 \times 10^6$ | $0.40 \times 10^6$ | 4 | $0.30 \times 10^6$ | $0.20 \times 10^6$ | 2 |

**Table 2-3:** Cell seeding densities and amount of cell culture medium used prior to transfection of the respective cell lines.

| **Cell lines** | **Seeding density/well in a 6-wp for 48 h treatment (number of cells)** | **Seeding density/well in a 6-wp for 72 h and 96 h treatment (number of cells)** | **Cell culture medium for 6-wp (ml)** | **Seeding density/well in a 12-wp for 48 h treatment (number of cells)** | **Seeding density/well in a 12-wp for 72 h and 96 h treatment (number of cells)** | **Cell culture medium for 12-wp (ml)** |
|---|---|---|---|---|---|---|
| ABC-1 | $0.40 \times 10^6$ | $0.32 \times 10^6$ | 4 | $0.20 \times 10^6$ | $0.16 \times 10^6$ | 2 |
| COLO320DM | $0.40 \times 10^6$ | $0.32 \times 10^6$ | 4 | $0.20 \times 10^6$ | $0.16 \times 10^6$ | 2 |

**Cyropreservation of cells**

1. Trypsinated to detach cells from a 175 $cm^2$ flask.
2. Transferred cells to a 50 ml tube containing 10 ml cell culture medium.
3. Spinned cells at 2000 rpm for 3 min.
4. Discarded supernatant.
5. Resuspended cells in cell culture medium containing 10% *(v/v)* dimethyl sulfoxide (DMSO).
6. Distributed cell culture in NUNC tubes for freezing at -70 ˚C in the Cyro freezing container (NAGLENE$^{TM}$).
7. Transferred cells in the liquid nitrogen tank, for long term storage.

## 2.1 Cell Treatments

### G007-LK treatment

10 mM of G007-LK stock solution was prepared in pre-warmed DMSO and kept at 4 °C for up to four weeks. 1µM of dilution was prepared in cell culture medium immediately before use. Dilutions with concentrations 0.33 µM, 0.1 µM and 0.033 µM were prepared according to the table 2-4, to keep equal amounts of DMSO in all the dilutions. 0.01% DMSO was used as vehicle and negative control.

**Table 2-4:** Exemplifying amounts of 1µM G007-LK and 0.01% DMSO solutions used to prepare the following dilutions of G007-LK.

| **Dilutions** | **0.33 µM** | **0.1 µM** | **0.033 µM** |
|---|---|---|---|
| 1 µM G007-LK in cell culture medium (ml) | 3.3 | 1 | 0.33 |
| 0.01% DMSO in cell culture medium (ml) | 6.7 | 9 | 9,67 |
| Total (ml) | 10 | 10 | 10 |

### esiRNA transfections

Endoribonuclease-prepared small interfering ribonucleic acids (esiRNAs) were used for degradation of target messenger ribonucleic acid (mRNA) *in vitro* [73].

*Procedure:*

1. Harvested, counted and seeded cells (see section 2.1.1) in a 12-wp and a 6-wp for each cell line as mentioned in Table 2-2 and 2-3.
2. The next day, after the cells had attached to the plates, the medium was changed in amounts mentioned in Table 2-5.
3. Mixed esiRNA, transfection buffer and tranfection reagent Pepmute Plus and incubated for 15 min.
4. Added the treatment in droplets to the respective wells. Transfection buffer and tranfection reagent Pepmute Plus were also used as vehicle and control in addition to control esiRNA targeting EGFP. The amounts of esiRNA, transfection buffer and transfection reagent Pepmute plus used for tranfections are listed in Table 2-5.

**Table 2-5:** Amounts of solutions used for esiRNA transfection

| Culture dish | Cell culture medium (ml) | Transfection buffer (µl) | 50 nM esiRNA (µl) | 25 nM esiRNA (µl) | Pepmute Plus (µl) |
|---|---|---|---|---|---|
| 12-wp | 0.75 | 75 | 2.8 | 1.4 | 3.3 |
| 6-wp | 1 | 100 | 3.6 | 2.8 | 4.0 |

## 2.2 The IncuCyte machine and MTS cell proliferation assay

The IncuCyte machine (Essens Bio Science) is used to capture images of growing cell cultures and process cell proliferation data.

The CellTiter 96® $AQ_{ueous}$ Non-Radioactive Cell Proliferation Assay or [3-(4,5-dimethylthiazol-2-yl)-5-(3-carboxymethoxyphenyl)-2-(4-sulfophenyl)-2H-tetrazolium, inner salt] (MTS) cell proliferation assay is a colorimetric technique used to determine the amount of living cells. The assay uses a substrate tetrazolium compound MTS and an electron coupling reagent phenazine methosulphate (PMS). MTS is converted into formazan by dehydrogenase enzymes found in living cells. Since formazan is easily soluble in cell medium, its absorbance can be measured. The number of viable cells in culture is directly proportional to the amount of formazan produced [74].

*Procedure:*

The cells were seeded in a 96-wp as listed in Table 2-6 and incubated at 37 °C with 5% $CO_2$. The next day, the cell culture medium was exchanged to solutions with increasing concentrations of G007-LK (0.033 µM, 0.1 µM, 0.33 µM or 1 µM) or vehicle 0.01% DMSO (control) and placed in the IncuCyte machine (at 37 °C with 5% $CO_2$). For each sample, there were at least 6 replicates. The IncuCyte machine was set to take pictures of the wells every second hour to examine the confluence of each well. The cells were incubated in the IncuCyte until the 0.01% DMSO treated control cells exited exponential growth phase (4 -10 days). The average of measured cell confluence for each replicate was calculated and plotted against the time elapsed.

NB! For SW480 cells increasing concentrations of G007-LK (0.1 µM, 1 µM or 5 µM) or vehicle 0.05% DMSO was used, while rest of the followed procedure for the incucyte machine proliferation assay was same as above.

**Table 2-6:** Adjusted cell seeding densities per 96-wp for the respective cell lines.

| Cell line | Cell seeding density per well |
|---|---|
| ABC-1 | 5000 |
| COLO320DM | 2500 |
| OVCAR-4 | 1000 |
| SW480 | 1000 |
| A-498 | 500 |

When the 0.01% DMSO treated control cells exited exponential growth phase as measured by the IncuCyte machine, the cell culture medium was exchanged with 20 µl substrate (5% PMS and 95% MTS) in 100 µl phenol free D-MEM solution. In parallel, during cell seeding minimum of six wells were seeded in replicates defining incubation time 0 ($t_0$), and the next day the cell culture medium was exchanged with 20 µl substrate in 100 µl phenol free D-MEM solution. The plates were incubated at 37 °C with 5% $CO_2$ for 1 h. After 1 h, absorbance (Abs) was measured at 490 nm with a microplate reader (FLUO Star Omega). The cell viability percentage relative to the control (0.01% DMSO) was calculated using the following formula: ((Sample $Abs_{490\ nm}$ -Average $Abs_{490\ nm\ t0}$)*100)/(Average $Abs_{490\ nm}$ 0.01% DMSO controls- Average $Abs_{490\ nm\ t0}$). The mean and standard deviation (SD) of relative cell viability percentage for each sample replicates was calculated and plotted as a histogram.

## 2.3 Working with quantitative real time polymerase chain reaction

Total RNA was extracted from the samples, and complementary deoxyribonucleic acid (cDNA) was synthesized to perform a two-step quantitative real time polymerase chain reaction (qRT-PCR).

**Total RNA extraction**

To extract total ribonucleic acid (RNA) GenElute$^{TM}$ mammalian total RNA miniprep kit (Sigma) was used. The protocol for adherent cells total RNA extraction was followed according to the supplier's recommendations. The quality and concentration of the extracted RNA was determined using a NanoDrop 2000c (Thermo Scientific) at $Abs_{260\ nm}$ and $Abs_{280\ nm}$. The $Abs_{260\ nm}/Abs_{280\ nm}$ ratio was always between 1.8 and 2.1.

**cDNA synthesis**

The complementary deoxyribonucleic acid (cDNA) was synthesized from messenger RNA (mRNA) template of the samples using SuperScript VILO cDNA synthesis kit (Invitrogen). This kit is designed to produce cDNA to be used in a qRT-PCR reaction. The supplier's

protocol was followed to synthesize cDNA. The synthesized cDNA was diluted 10 fold before use in the qRT-PCR.

**Quantitative real time polymerase chain reaction**

Quantitative real time polymerase chain reaction (qRT-PCR) is a technique that not only amplifies the target DNA region but also calculates the product at each cycle. The DNA is amplified in the same way as in the conventional polymerase chain reaction (PCR). But the fluorescent resonance energy transfer (FRET) technology and 5'exonuclease activity of the TaqMan DNA polymerase makes it more specific than the conventional PCR. And the amplified target DNA product is quantified in real time without any post PCR assays.

qRT-PCR assay is usually run for 40 cycles. Each cycle consists of three main steps.

- Denaturing of the double stranded DNA at 95 ˚C.
- Annealing of primers and probes to the target region at 60 ˚C.
- TaqMan DNA polymerase activity at 60 ˚C.

Double stranded DNA is denatured at high temperature of 95 °C. The temperature is then sunk so that annealing of primer and probe to the target region can take place. Once primer is annealed to the target region, Taqman polymerase attaches at the 3' region of the primer and extends it. When Taqman polymerase encounters the hybridized probe at the 5', it exerts 5'nuclease activity. The reporter is then cleaved from the quencher and emits signal upon light exposure that is captured by the machine. The amount of fluorescence produced from the reporter is directly proportional to the amount of the amplicon produced in the cycle.

**Comparative quantification algorithms $\Delta\Delta C_t$** method was used for quantification of the target genes in the samples. The treated samples were compared with the untreated sample to test the expression of genes. Glyceraldehyde phosphate dehydrogenase (GAPDH) was used as the endogenous sample loading control. Fold difference in the expression of target (gene of interest) between "untreated sample" and "treated sample" is given by the following formula $2^{-\Delta\Delta Ct}$.

$C_t$ is the threshold cycle number. It is the cycle number when the fluorescent signal is significantly higher than the baseline (background) signal. The lower the $C_t$ value, the higher is the starting amount of the target [75].

$$\Delta\Delta C_t = (C_{t\ GOI}{}^{S} - C_{t\ norm}{}^{S}) - (C_{t\ GOI}{}^{C} - C_{t\ norm}{}^{C}) *$$

* $C_{t\ GOI}{}^{S}$: threshold cycle number of the gene of interest in the treated sample; $C_{t\ norm}{}^{S}$: threshold cycle number of the GAPDH in the treated sample; $C_{t\ GOI}{}^{C}$: threshold cycle number of the gene of interest in the untreated sample; $C_{t\ norm}{}^{C}$: threshold cycle number of the GAPDH in the untreated sample.

*Procedure:*

According to the supplier's recommendations, cDNA template along with TaqMan gene expression reagents and RNase-free water was used to prepare qRT-PCR reaction mix. qRT-PCR was run on Applied Biosystems ViiA7 real-time PCR system (Life technologies) for 40 cycles and $\Delta\Delta C_t$ method was used for data analysis.

## 2.4 Western blotting

Western blotting (WB) technique is used to detect and analyze specific target proteins in the samples. The technique includes the following steps: i) Cell lysates preparation with appropriate lysis buffer, ii) Protein quantification with the Bradford assay, iii) SDS gel electrophoresis for protein separation, iv) Protein electrotransfer on the PVDF membrane and v) Target protein detection through target protein specific antibodies.

### Preparation of cell lysates

Cells grown in a 6-wp were lysed in chilled 100 µl of lysis buffer (Appendix 3) and placed on ice for about 30 min. Using cell scraper, the cells were scraped and collected into one corner of the well and re-suspended by pipetting up and down. The cell lysate was transferred into a new eppendorf tube and spinned at 15000 rpm for 15 min at 4 °C. Membrane cytoplasmic fraction was separated from the pelleted nuclei.

For nuclei pellet lysis, 100 µl of 1xRIPA buffer (Appendix 3) was added. The nuclei pellet with 1xRIPA buffer was run on the sonicator machine Bioruptor (Diagenode) for 10 min (30 seconds ON/OFF cycles).

### Quantification of proteins with the Bradford assay

Bradford assay is used to measure the protein concentration in samples. Bovine serum albumin (BSA) was used as a protein standard. BSA and protein extract dilutions were prepared in Quick start™ Bradford 1x Dye Reagent and the absorbance was measured at 595 nm with the spectrophotometer. 1 ml of Quick start™ Bradford 1x Dye Reagent was used as a blank. BSA measurements with different concentrations (1-9 µg/µl) were used to prepare a standard curve. The protein concentration in the sample was determined using the linear regression equation from the standard curve.

### Separation of proteins with the SDS-PAGE

Sodium dodecyl sulfate-polyacrylamide gelelectrophoresis (SDS-PAGE) separate proteins based on their molecular weights when electric current is applied. For separation of larger proteins, polyacrylamide gels with a lower percentage of acrylamide were used. For improved separation of small and large proteins, gradient gels were used. In a gradient gel the upper part of the gel has a lower percentage of acrylamide, while the lower part of the gel has a larger percentage of acrylamide. In this way, a wide range of proteins sizes can be separated in a single gel [76].

*Procedure:*

SDS loading buffer (4X) (Appendix 3) was mixed with protein samples. The protein samples were then boiled at 85 ˚C for about five min. 25 µl of the protein samples, with equal protein concentration, were loaded in the wells of precast polyacrylamide gels (NuPage). The gels were run at 20 mA per gel for 2 h in a XCell SureLock$^{TM}$ electrophoresis cell (Invitrogen). See Appendix 3 for all buffers and solutions used in SDS-PAGE.

### Protein transfer to the PVDF membrane

The proteins were transferred from the polyacrylamide gel to the polyvinylidene difluoride (PVDF) membrane with a Trans-Blot® SD semi-dry electrophoretic transfer cell (Bio-Rad). The gel, PVDF membrane and filter paper were first soaked in transfer buffer (Appendix 3) for 10 min to reach equilibration. A sandwich was prepared in the following order from anode to cathode: Filter paper, PVDF membrane, protein gel, filter paper. Electrotransfer of proteins, from the gel to PVDF membrane, was done at 500 mA per gel overnight. See Appendix 3 for all buffers and solutions used.

### Protein detection with antibodies

To prevent unspecific binding, the PVDF membrane must be blocked with a blocking buffer prior to protein detection. The membrane was blocked with 5% nonfat dried milk in tris-buffered saline tween (TBS-T) or 5% BSA in TBS-T. The membrane was then incubated with the primary antibody over night. See Appendix 2 for all antibodies used. After optimized number of wash steps, the membrane was incubated with a HRP-conjugated-secondary antibody with affinity for the primary antibody. The membrane was again washed to remove unbound antibody and then incubated in enhanced chemiluminescent (ECL) solution for 3 min. Light is emitted when the HRP enzyme reacts with a chemiluminescent substrate and can be detected by a light sensitive film or a camera. The bands produced depict the target proteins specific for the antibody used. A developer machine (AGFA) or a gel imaging cabinet (Bio-Rad) was used to detect protein bands. ACTIN was used as loading control. See Appendix 3 for all buffers and solutions used in WB.

## 2.5 Statistical analyses

SigmaPlot® 12.5 (Systat Software Inc.) was used for statistical analyses. Normal distribution of the datasets to be compared was tested with Shapiro-Wilk test prior to the Student t-test. The Student t-test was performed if the Shapiro-Wilk test passed (P=>0.05). Mann-Whitney rank sum test was performed if the Shapiro-Wilk test failed (P=<0.05). For both, Student t-test and Mann-Whitney rank sum test, the statistical significant difference was set to be $P<0.05$ [48].

# 3. Results

## 3.1 Treatment response of G007-LK on the cancer cell lines

The project aimed to validate if the cancer cell lines ABC-1, OVCAR-4, A498, COLO320DM and SW480 are G007-LK-sensitive. G007-LK-sensitive cell lines may display at least one of the following features: i) TNKS1/2 inhibition (usually observed as differently expressed TNKS1/2 protein levels), ii) Increased AXIN protein levels, iii) Decreased WNT pathway signaling and iv) Reduced proliferation [4]. Furthermore, the aim was also to explore BMF as a potential biomarker in response to G007-LK treatment, and investigate a potential interplay between AXIN, AMPK and BMF.

### 3.1.1 Growth inhibition analysis upon G007-LK treatment in the cancer cell lines

The Incucyte machine proliferation assay was executed to validate the growth inhibitory effect of G007-LK treatment on cell growth of ABC-1, COLO320DM, OVCAR-4, SW480 and A-498, while MTS proliferation was conducted only in ABC-1, COLO320DM and OVCAR-4. The results indicated that G007-LK had a growth inhibitory effect on ABC-1, COLO320DM and OVCAR-4 with a concentration of 0.1, 0.33 and 1 µM ($P<0.05$)(Fig. 3-1, A and B). In the SW480 cells, significant growth inhibition was observed with a G007-LK concentration of 0.1 µM, 1 µM and 5 µM ($P<0.05$)(Fig. 3-1, C, left). The growth inhibition in A-498 cell line upon G007-LK exposure was not found to be statistically significant (Fig. 3-1, C, right).

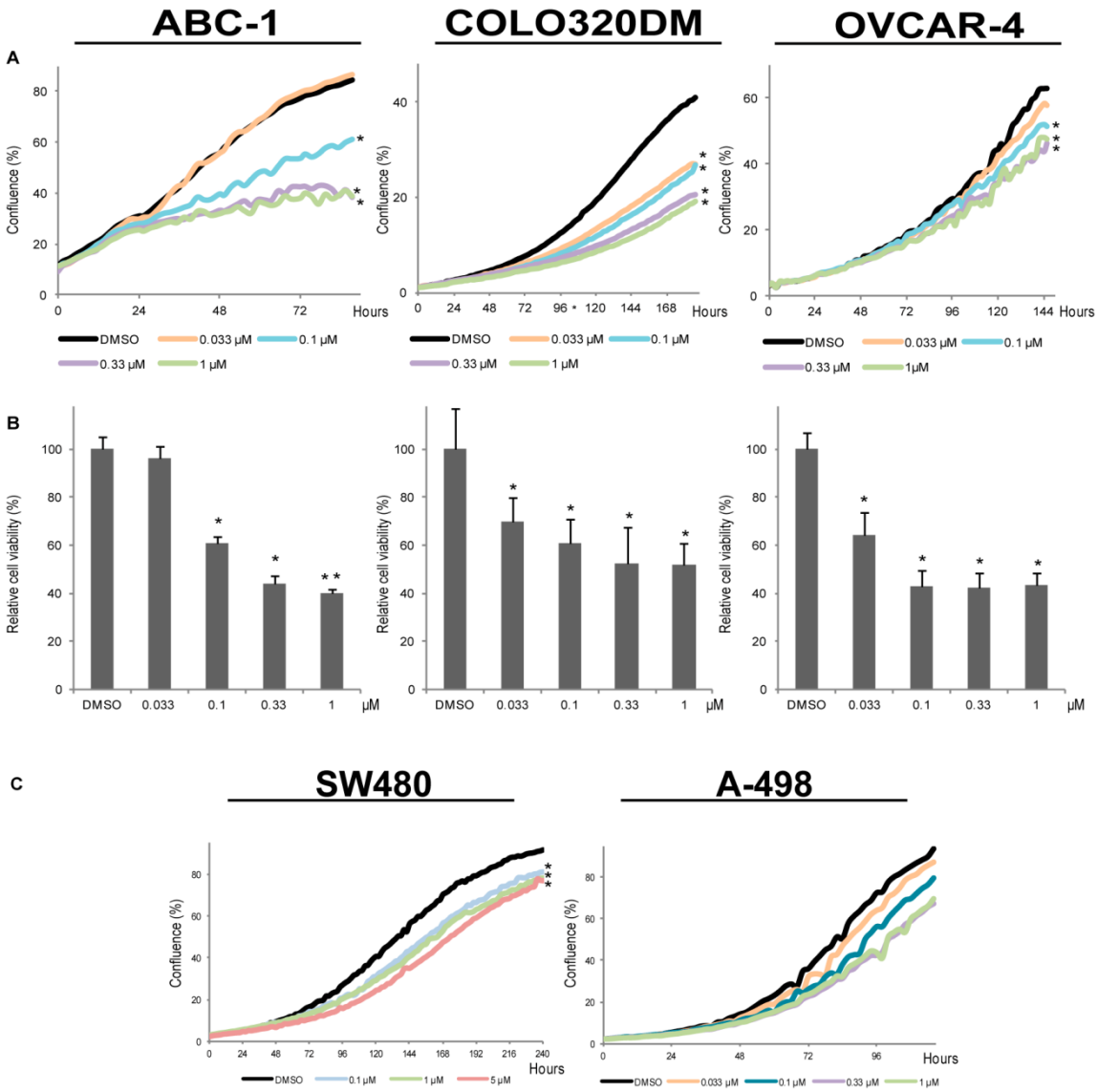


**Figure 3-1:** Inhibition of cell proliferation in ABC-1, COLO320DM, OVCAR-4 and SW480 upon G007-LK exposure in a concentration-dependent manner. The cells were exposed with the indicated concentrations of G007-LK or vehicle DMSO (control) for the indicated hours. * indicates statistical significance difference P< 0.05 between control and treated samples upon calculation by the Student t-test. ** indicates statistical significance difference P< 0.05 between control and treated samples upon calculation by the Rank Sum test. A, Cell growth curve as measured by the IncuCyte machine shows a G007-LK concentration-dependent significant decrease of proliferation in ABC-1, COLO320DM and OVCAR-4. B, MTS assay showing G007-LK concentration-dependent viability decrease in ABC-1, COLO320DM and OVCAR-4. C, left, cell growth curve as measured by the IncuCyte machine shows a G007-LK concentration-dependent significant decrease of proliferation in SW480. C, right, in A-498, cell growth curve as measured by the IncuCyte machine does not show a statistically significant decrease in proliferation upon G007-LK treatment. The mean values and the standard deviation (SD) of several measurements are shown.

### 3.1.2 G007-LK treatment response on the protein TNKS1/2, the WNT pathway and *BMF* in the selected cancer cell lines

The cancer cell lines SW480, OVCAR-4, A-498, ABC-1 and COLO320DM were treated with 1 µM G007-LK or 0.01% DMSO (control) for 24 h or 72 h to see the G007-LK treatment response on the protein TNKS1/2, the WNT pathway and *BMF*.

#### Quantitative real time polymerase chain reaction analysis

A qRT-PCR was used to analyze both *BMF* and *AXIN2* mRNA levels upon G007-LK exposure relative to DMSO.

- In the 24 h G007-LK treated samples, *BMF* mRNA was significantly upregulated in all the tested cell lines ($P<0.05$)(Fig. 3-2A, left panel).
- In the 72 h G007-LK treated samples *BMF* mRNA was significantly upregulated in all the tested cell lines ($P<0.05$) except for A-498 (Fig. 3-2A, right panel).
- Both the 24 h and 72 h G007-LK treated samples, showed a significant decrease of *AXIN2* mRNA in SW480, OVCAR-4 and COLO320DM (Fig. 3-2A).

#### Western blot analysis

In order to determine the G007-LK treatment response at the functional level, WB analyses was conducted. Cytoplasmic fractions extracted from SW480, OVCAR-4, A-498 and ABC-1 cells were analyzed by WB using antibodies against AXIN1, TNKS1/2, ABC, total β-catenin and ACTIN. Data were normalized to ACTIN expression.

**ABC-1**

Elevated AXIN1 and declined TNKS1/2 protein levels were observed at both 24 h and 72 h of G007-LK exposure in ABC-1. In addition, a moderate decrease in ABC levels was observed only at 72 h of G007-LK treatment but total β-catenin levels were not decreased (Fig. 3-2B).

**OVCAR-4**

Upregulated AXIN1 and down-regulated TNKS1/2 protein levels were observed in OVCAR-4 only at 72 h of G007-LK exposure. Additionally, ABC levels were increased but no substantial effect was observed on total β-catenin levels in OVCAR-4 (Fig. 3-2B). NB! OVCAR-4 gel was accidentally cut, at the AXIN1 and ABC protein bands position, for the 24 h treated sample.

**SW480**

Enhanced AXIN1 and diminished TNKS1/2 protein levels were observed in SW480 at both 24 h and 72 h of G007-LK treatment. Simultaneously, both ABC and total β-catenin levels were strongly decreased in SW480 (Fig. 3-2B).

**A-498**

Increased AXIN1 and decreased TNKS1/2 protein levels were observed at both the 24 h and 72 h of G007-LK exposure in A-498. However, ABC protein levels were moderately decreased only in the 72 h G007-LK treated sample but no effect was observed on the total β-catenin protein levels (Fig. 3-2B).

Of all the cell lines tested, 72 h of G007-LK exposure exhibited TNKS1/2 inhibition and AXIN1 protein stabilization (Fig. 3-2B and 3-4B). Simultaneously, ABC protein levels were strongly decreased in SW480 (Fig. 3-2B) and COLO320DM (Fig. 3-4B) but moderately decreased in ABC-1 and A-498 (Fig. 3-2B). In OVCAR-4, ABC protein levels were elevated upon 72 h of G007-LK exposure. However, WNT pathway target gene down-regulation was observed only in SW480, OVCAR-4 and COLO320DM. Additionally, *BMF* mRNA was upregulated in ABC-1, COLO320DM, OVCAR-4 and SW480 cells for 24 h and 72 h of G007-LK exposure. In A-498 cells, an upregulation of *BMF* mRNA was only observed at 24 h (Fig. 3-2A).

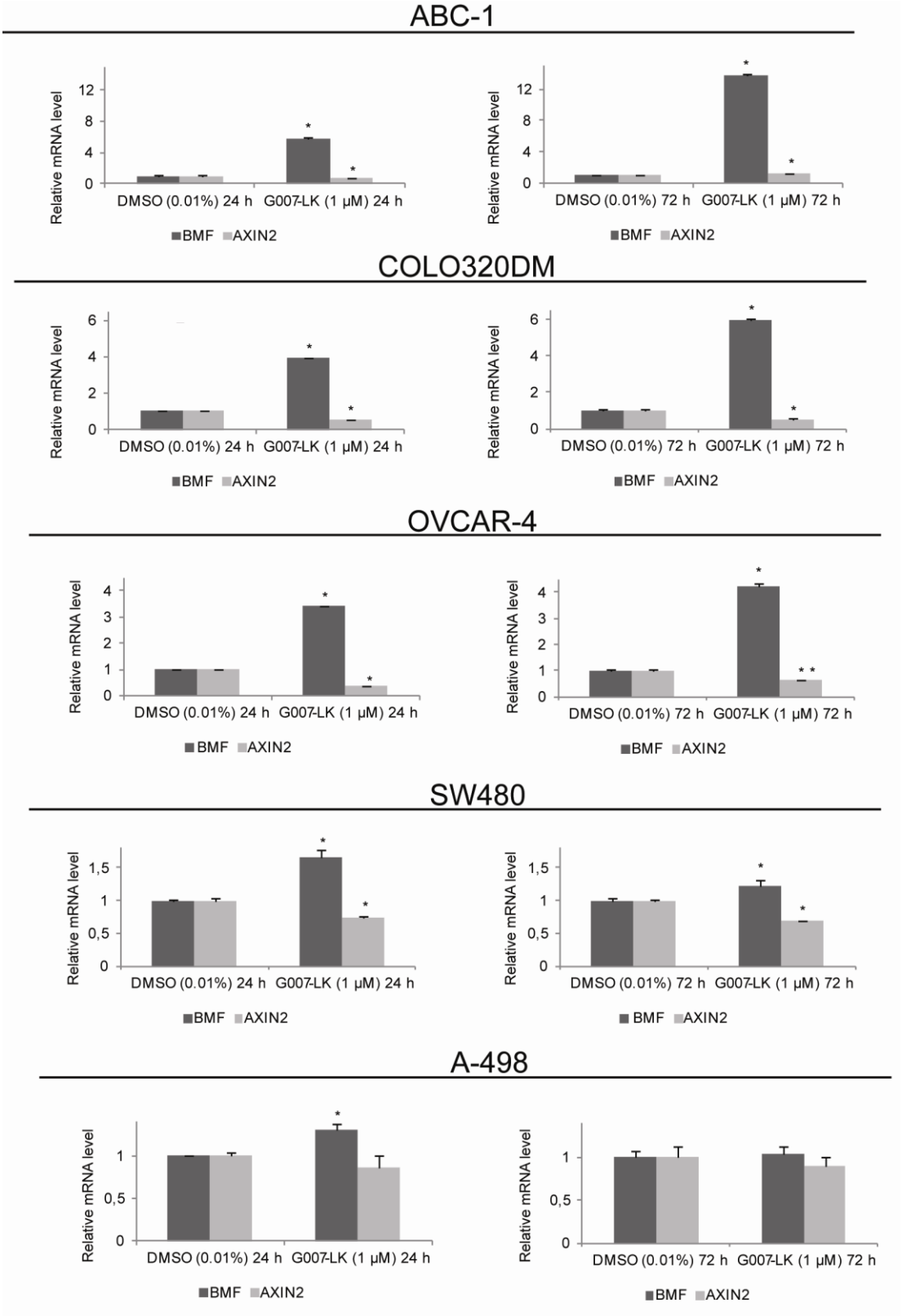


**Figure 3-2A:** A qRT-PCR representing relative increase of *BMF* mRNA in SW480, OVCAR-4, A-498, ABC-1 and COLO320DM after G007-LK exposure. The cells were treated with 1 µM G007-LK or 0.01% DMSO (control) for 24 h or 72 h. Data was normalized to GAPDH and is relative to DMSO-treated samples. The mean values of three replicates with SD are shown. * represents statistical significance difference P<0.05 upon calculation with the Student t-test. ** represents statistical significance difference P<0.05 upon calculation with the Rank Sum test. *BMF* mRNA was significantly increased in SW480, OVCAR-4, ABC-1 and COLO320DM upon G007-LK exposure for 24 h and 72 h (P<0.05), however, in A498 *BMF* mRNA was significantly increased at only 24 h of G007-LK exposure (P<0.05). *AXIN2* mRNA was significantly decreased in SW480, COLO320DM and OVCAR-4 upon G007-LK exposure for 24 h and 72 h (P<0.05).

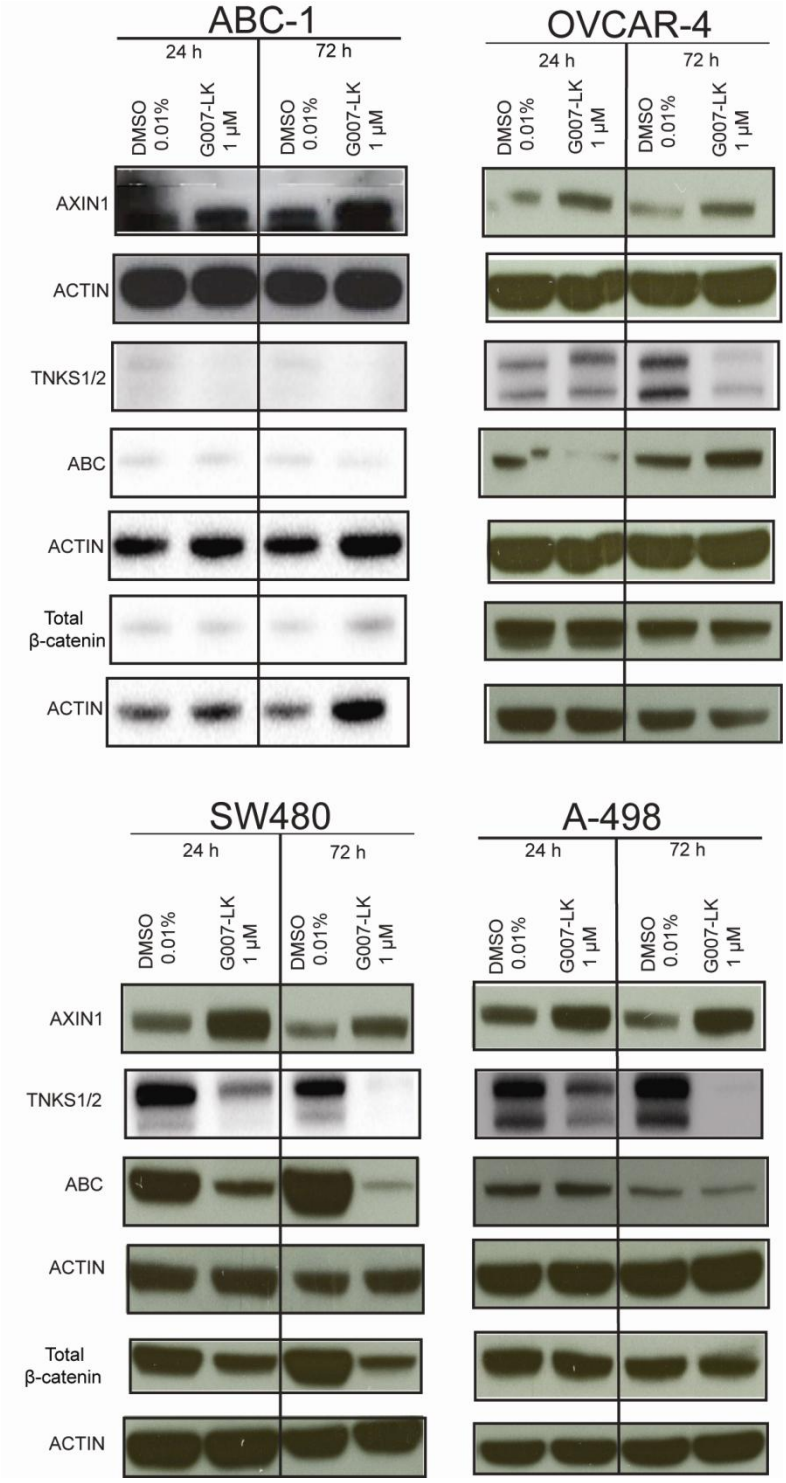


**Figure 3-2B:** A WB analysis representing decrease of TNKS1/2 and upregulation of AXIN1 upon G007-LK exposure in the cytoplasmic fractions of SW480, OVCAR-4, A-498 and ABC-1. The cells were treated with 1 µM G007-LK or 0.01% DMSO (control) for 24 h or 72 h. Cytoplasmic fractions were analyzed by WB using antibodies against AXIN1, TNKS1/2, ABC, total β-catenin and ACTIN. Data were normalized to ACTIN expression.

## 3.2 Interplay between AXIN1, AMPK and *BMF* upon treatment with the TNKS1/2 inhibitor G007-LK

The previous experiments suggested that *BMF* transcription is strongly upregulated upon G007-LK treatment in ABC-1 and COLO320DM (Fig. 3-2A). The AMPK-activation pathway was chosen to explore a potential interplay between AXIN1, AMPK and BMF upon treatment with G007-LK, because we found strong potential links between AXIN, AMPK activation and BMF in literature [4][6][72]. We hypothesized that G007-LK mediated AXIN stability enhances formation of AMPK activation complex LKB1-AXIN-AMPK, and mediates AMPK activation. Activated AMPK causes upregulation of *BMF* transcription (Fig. 1-10). The cells were treated with [25 nM *AMPKα1* + 25 nM *AMPKα2* (50 nM *AMPKα)*] esiRNA, 50 nM *BMF* esiRNA, 50 nM control (Ctrl) esiRNA or no esiRNA and vehicle (10% transfection buffer, 0.4% Pepmute and cell culture medium) for 24 h. The transfection was followed by the addition of 1µM G007-LK treatment or vehicle (0.01% DMSO) for the last 48 h or 72 h.

### Quantitative real time polymerase chain reaction analysis in ABC-1

The qRT-PCR analysis indicated the following results in the ABC-1 (Fig. 3-3A):

*AMPKα1* mRNA was knocked down in the *AMPKα1* esiRNA treated samples ($P<0.05$)(Fig. 3-3A, a). *AMPKα2* transcription was knocked down only in the 96 h *AMPKα2* esiRNA treated samples ($P<0.05$)(Fig. 3-3A, b, right). *BMF* transcription was down-regulated in the *BMF* esiRNA treated samples ($P<0.05$)(Fig. 3-3A, d and e).

#### *AMPKα1*

The *BMF* esiRNA treated samples displayed no affect on the *AMPKα1* transcription, compared to the control (Ctrl esiRNA + DMSO), ($P<0.05$)(Fig. 3-3A, a). However, *AMPKα1* mRNA was strongly elevated in the G007-LK treated samples, compared to the control ($P<0.05$)(Fig. 3-3A, a).

#### *AMPKα2*

The *BMF* esiRNA treated samples displayed no affect on the *AMPKα2* transcription, compared to the control ($P<0.05$)(Fig. 3-3A, b). However, *AMPKα2* mRNA was strongly elevated in the G007-LK treated samples, compared to the control ($P<0.05$)(Fig. 3-3A, b).

#### *AXIN2*

The *AMPKα* esiRNA treated samples showed moderate increase in *AXIN2* mRNA levels, compared to the control (Ctrl esiRNA + DMSO)($P<0.05$)(Fig. 3-3A, c). A mild to moderate increase of *AXIN2* transcription was also observed in the only 72 h of G007-LK treated samples, compared to the control ($P<0.05$)(Fig. 3-3A, c, right). Compared to the G007-LK treated sample, a significant increase of the *AXIN2* transcription was displayed in the

combined treatment sample (96 h *AMPKα* esiRNA + 72 h G007-LK)($P<0.05$)(Fig. 3-3A, c, right).

***BMF***

*BMF* mRNA was moderately upregulated in the 96 h *AMPKα* esiRNA sample, compared to the control (Fig. 3-3A, e, right). However, *BMF* transcription was strongly upregulated in the G007-LK treated samples (Fig. 3-3A, d). Furthermore, G007-LK exposure in the *BMF* esiRNA treated sample retrieved *BMF*, compared to the just *BMF* esiRNA treated sample (Fig. 3-3A, d).

## Western blot analysis in ABC-1

AXIN1 levels were enhanced and TNKS1/2 levels were decreased in the G007-LK treated samples, compared to their relative none-G007-LK treated samples. In addition, both ABC and total β-catenin levels were moderately reduced (Fig. 3-3B). The G007-LK treated sample displayed no substantial affect on the p-AMPKα (Thr172) protein levels, compared to the control (Ctrl + DMSO)(Fig. 3-3B).

AMPKα protein levels were decreased in the *AMPKα* esiRNA treated sample, compared to the control (Fig. 3-3B) .

The *AMPKα* and *BMF* esiRNA treated samples displayed no substantial affect on the protein levels of AXIN1 and TNKS1/2, compared to the control. However, ABC protein levels were moderately increased. Furthermore, the *BMF* esiRNA treated sample showed increased p-AMPKα (Thr172) protein levels, compared to the control (Fig. 3-3B).

To sum up, ABC-1 displays TNKS1/2 inhibition and AXIN1 stabilization upon G007-LK exposure (Fig. 3-3B). Moreover, ABC protein levels were moderately decreased but WNT pathway target gene, *AXIN2*, was mildly to moderately upregulated (Fig. 3-3B and 3-3A, c). Therefore, if ABC-1 is WNT pathway inhibition sensitive in response to G007-LK remains elusive. *BMF* transcripts were strongly upregulated upon G007-LK exposure (Fig. 3-3A). However, BMF protein levels could not be reliably detected by any of the commercially available antibody. *AXIN2* mRNA was elevated upon 96 h of *AMPKα* and *BMF* esiRNA treatment (Fig. 3-3A, c). Simultaneously, a moderate increase in the ABC protein levels was observed (Fig. 3-3B). *BMF* esiRNA treatment raised p-AMPKα (Thr172) protein levels (Fig. 3-3B). However, G007-LK-mediated AXIN1 stability displayed no substantial effect on the p-AMPKα (Thr172) protein levels and AMPKα (Fig. 3-3B).

The hypothesis that G007-LK-mediated AXIN stability enhances AMPK activation, and AMPK activation maybe leads to *BMF* transcriptional upregulation, could not be validated in the ABC-1 cells.

## Quantitative real time polymerase chain reaction analysis in COLO320DM

The qRT-PCR analysis indicated the following results in the COLO320DM:

*AMPKα1* and *AMPKα2* mRNA was knocked down in the *AMPKα* esiRNA treated samples ($P<0.05$)(Fig. 3-4A, a and b). *BMF* mRNA was knocked down in the *BMF* esiRNA treated samples ($P<0.05$)(Fig. 3-4A, d and e).

### *AMPKα1*

The only 48 h G007-LK treated sample displayed a moderate decline in the *AMPKα1* mRNA, compared to the control sample (Ctrl esiRNA +DMSO)($P<0.05$)(Fig. 3-4A, a, left). However, a moderate increase of the *AMPKα1* transcription was observed in the 72 h G007-LK treated sample, compared to the control sample (no esiRNA + DMSO)($P<0.05$)(Fig. 3-4A, a, right).

The only 96 h *BMF* esiRNA treated sample showed elevated transcription of *AMPKα1*, compared to the control sample (no esiRNA +DMSO)($P<0.05$)(Fig. 3-4A, a, right).

### *AMPKα2*

Compared to the control (Ctrl esiRNA + DMSO), the only 48 h G007-LK treated sample displayed a moderate decrease in *AMPKα2* mRNA ($P<0.05$)(Fig. 3-4A, b, left). However, no significant difference was observed at 72 h of sole G007-LK treatment compared to the control (no esiRNA + DMSO)(Fig. 3-4A, b, right).

The only 96 h of *BMF* esiRNA treated sample displayed moderately upregulated *AMPKα2* mRNA, compared to the control (no esiRNA + DMSO)($P<0.05$)(Fig. 3-4A, b, right). Compared to the 72 h G007-LK treated sample, the combined treated sample (96 h *BMF* esiRNA + 72 h G007-LK) also displayed a mild to moderate increase in the *AMPKα2* mRNA ($P<0.05$)(Fig. 3-4A, b, right).

### *AXIN2*

The *BMF* and *AMPKα* esiRNA treated samples displayed no significant effect on *AXIN2* mRNA levels, compared to control samples ($P<0.05$)(Fig. 3-4A, c). However, G007-LK exposure significantly down-regulated *AXIN2* transcription in all the samples, compared to control samples. ($P<0.05$)(Fig. 3-4A, c).

### *BMF*

The *BMF* transcription was strongly upregulated in the G007-LK treated samples, compared to control samples ($P<0.05$)(Fig. 3-4A, d). Furthermore, G007-LK exposure in the *BMF* esiRNA treated sample retrieved *BMF*, compared to the sole *BMF* esiRNA treated sample ($P<0.05$)(Fig. 3-4A, d).

## Western blot analysis in COLO320DM

The WB analysis showed the following results in the COLO320DM.

AXIN1 levels were enhanced and TNKS1/2 levels were decreased in the G007-LK treated samples, compared to their relative none-G007-LK treated samples. In addition, both ABC and total β-catenin levels were strongly reduced. Simultaneously, phosphorylated-AMPKα-at-Thr172 [p-AMPKα (Thr 172)] protein levels were also increased (Fig. 3-4B).

Both the just *AMPKα* esiRNA and *BMF* esiRNA treated samples showed no substantial effect on the protein levels of AXIN1, TNKS1/2, ABC and total β-catenin, compared to the control (Ctrl esiRNA + DMSO), (Fig. 3-4B).

Both the AMPKα and p-AMPKα (Thr 172) protein levels were knocked down in the 96 h *AMPKα* esiRNA treated samples, compared to the control. However, G007-LK exposure retrieved p-AMPKα (Thr 172) protein levels (Fig. 3-4B, right).

BMF protein levels could not be determined due to poor commercially available antibodies. However, the 96 h *BMF* esiRNA treated sample displayed enhanced protein levels of AMPKα but decreased p-AMPKα (Thr 172), compared to the control (Fig. 3-4B, right).

To sum up, AXIN1 was enhanced and TNKS1/2 was decreased upon G007-LK exposure. Moreover, both ABC and total β-catenin protein levels were strongly reduced (Fig. 3-4B). The WNT pathway target gene, *AXIN2*, was also strongly inhibited upon G007-LK exposure (Fig. 3-4A, c). Therefore, COLO320DM displays both TNKS1/2 and WNT pathway inhibition upon G007-LK treatment, is validated. Moreover, total APMKα protein levels were unaltered but p-AMPKα (Thr 172) protein levels were increased upon G007-LK exposure (Fig. 3-4B, right). In contrast, total AMPKα levels were reduced by G007-LK treatment in *BMF* depleted cells, compared to cells treated with *BMF* esiRNA. However, still increased p-AMPKα (Thr172) protein levels were seen. In conclusion, tankyrase inhibition affected AMPKα protein levels only in the absence of *BMF*, again compared to cells treated with *BMF* esiRNA, but G007-LK increased p-AMPKα (at Thr172) protein levels independent of *BMF* (Fig. 3-4B, right). Simultaneously, *BMF* transcripts were strongly upregulated upon G007-LK exposure (Fig. 3-4A, d).

Since the protein levels of p-AMPKα (Thr 172) were increased upon G007-LK exposure (Fig. 3-4B), there are tendencies that G007-LK-mediated AXIN stability enhances AMPK activation, and AMPK activation maybe leads to *BMF* transcriptional upregulation, in the COLO320DM cells.

## Mini conclusion

COLO320DM is both TNKS1/2 and WNT pathway inhibitor sensitive in response to G007-LK (Fig. 3-4A, c and 3-4B). However, only TNKS1/2 inhibition could be confirmed in ABC-1 (Fig. 3-3B). Additionally, *BMF* transcription is strongly upregulated in COLO320DM (Fig. 3-4A, d) and much more strongly upregulated in ABC-1 (Fig. 3-3A, d) in response to G007-LK treatment. Since p-AMPKα (Thr 172) protein levels were increased upon G007-LK exposure in COLO320DM (Fig. 3-4B), but not in ABC-1(Fig. 3-3B), there are tendencies that G007-LK-mediated AXIN1 stability enhances AMPK activation in COLO320DM. This activation of AMPK may further lead to transcriptional upregulation of *BMF* in COLO320DM cells (Fig. 3-4B, right) but not in ABC-1 cells (Fig. 3-3B).

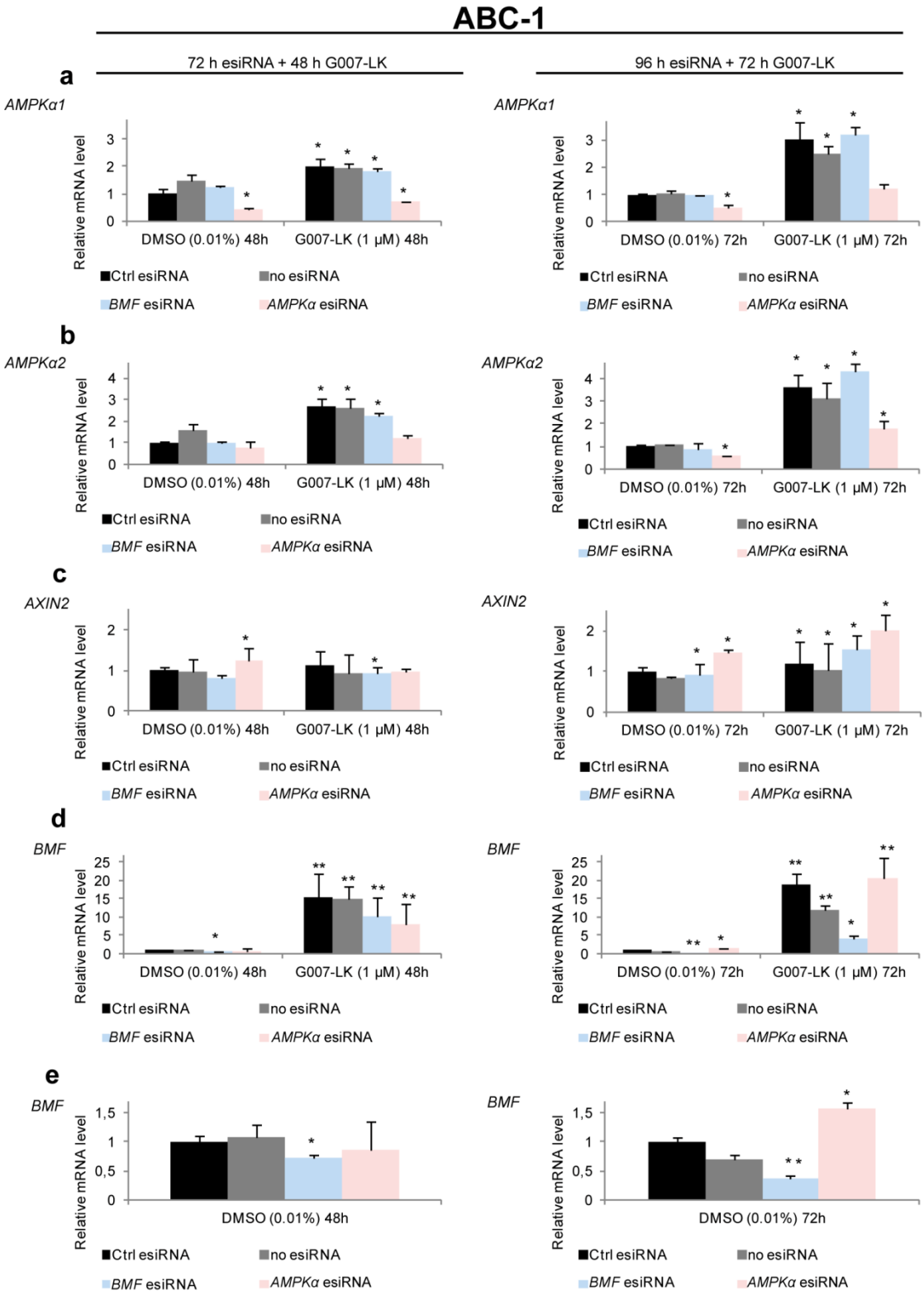


**Figure 3-3A:** A qRT-PCR analysis represents that G007-LK treatment in ABC-1 led to: i) Elevated mRNA levels of *BMF*, *AMPKα1* and *AMPKα2*. ii) Moderate to mild increase in *AXIN2* transcription for 72 h. The cells were treated with [25 nM *AMPKα1* + 25nM *AMPKα2* (*AMPKα* )]esiRNA , 50 nM *BMF* esiRNA, 50 nM control (Ctrl) esiRNA or no esiRNA and vehicle (10% transfection buffer, 0.4% Pepmute and cell culture medium) for 24 h. The transfection was followed by addition of 1 μM G007-LK treatment or vehicle (0.01% DMSO) for 48 h or 72 h. *AMPKα1*, *AMPKα2* , *BMF*, *AXIN2* and *GAPDH* mRNA levels were determined using qRT-PCR. Data were normalized to *GAPDH* levels and are relative to the control sample (Ctrl esiRNA + 0.01% DMSO). The mean values of at least three replicates and SD is shown. * represents statistical significance difference, P<0.05, between the control sample and the treated samples upon calculation with the Student t-test. ** represents statistical significance difference, P<0.05, between the control sample and the treated samples upon calculation with the Rank Sum test. The letters a, b, c, d and e symbolize result histograms for *AMPKα1*, *AMPKα2*, *AXIN2*, *BMF* and *BMF* respectively.

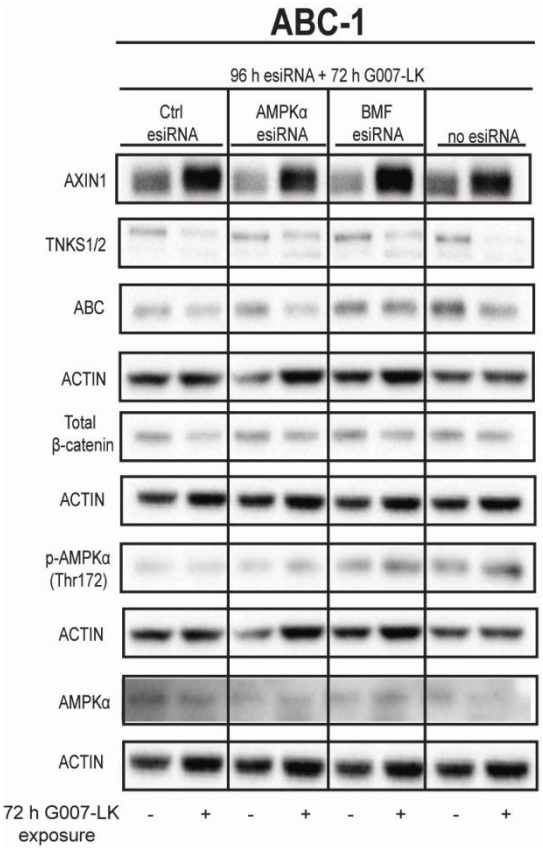


**Figure 3-3B:** The WB analysis represents that G007-LK exposure in ABC-1 led to the following: i) Increased AXIN1 protein expression upon TNKS1/2 inhibition. ii) Moderately decreased ABC protein expression. iii) No considerable effect on p-AMPKα (Thr172) levels. The cells were treated with [25 nM *AMPKα1* + 25nM *AMPKα2* (*AMPKα* )]esiRNA , 50 nM *BMF* esiRNA, 50 nM control (Ctrl) esiRNA or no esiRNA and vehicle (10% transfection buffer, 0.4% Pepmute and cell culture medium) for 24 h. The transfection was followed by addition of 1 μM G007-LK treatment or vehicle (0.01% DMSO) for 48 h or 72 h. Cytoplasmic fractions extracted from ABC-1 were analyzed by WB using antibodies against AXIN1, TNKS1/2, ABC, total β-catenin, p-AMPKα (Thr172), AMPKα and ACTIN (loading control).

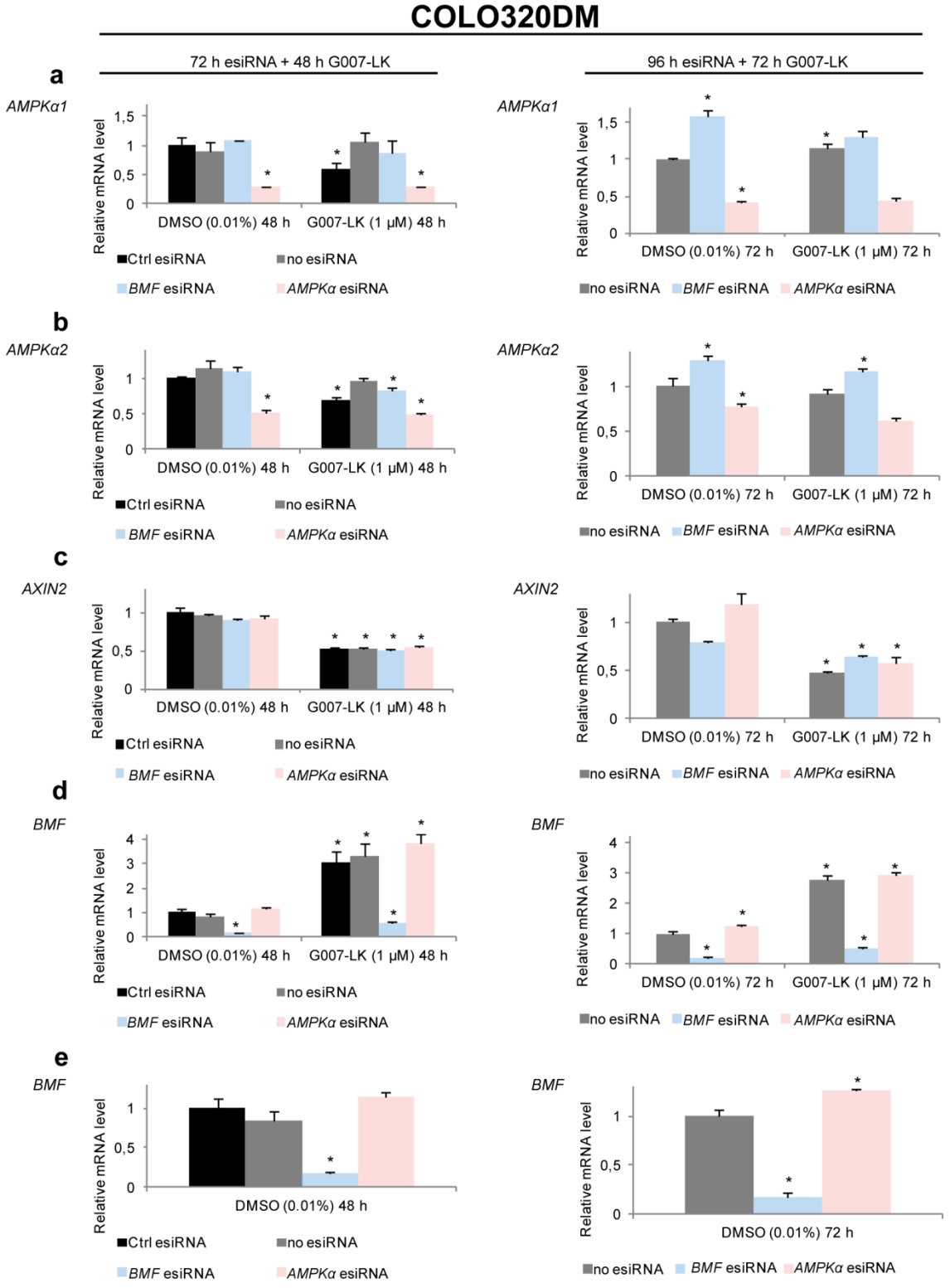


**Figure 3-4A:** A qRT-PCR analysis represents that G007-LK treatment in COLO320DM led to the following: i) Decreased *AXIN2* transcription. ii) Elevated *BMF* transcription. iii) *AMPKα1* transcription increased only upon 72 h of G007-LK exposure. The cells were treated with [25 nM *AMPKα1* + 25nM *AMPKα2* (*AMPKα* )]esiRNA, 50 nM *BMF* esiRNA, 50 nM control (Ctrl) esiRNA or no esiRNA and vehicle (10% transfection buffer, 0.4% Pepmute and cell culture medium) for 24 h. The transfection was followed by addition of 1 μM G007-LK treatment or vehicle (0.01% DMSO) for the last 48 h or 72 h. *AMPKα1*, *AMPKα2*, *BMF*, *AXIN2* and *GAPDH* mRNA levels were determined using qRT-PCR and data were normalized to *GAPDH* levels. The mean values of replicates and SD is shown. Left, data is relative to the control sample (Ctrl esiRNA + 0.01% DMSO). Right, data is relative to the control sample (no esiRNA + 0.01% DMSO).* represents statistical significance difference, P<0.05, between the control and the treated samples upon calculation with the Student t-test. The letters a, b, c, d and e symbolize result histograms for *AMPKα1*, *AMPKα2*, *AXIN2*, *BMF* and *BMF* respectively.

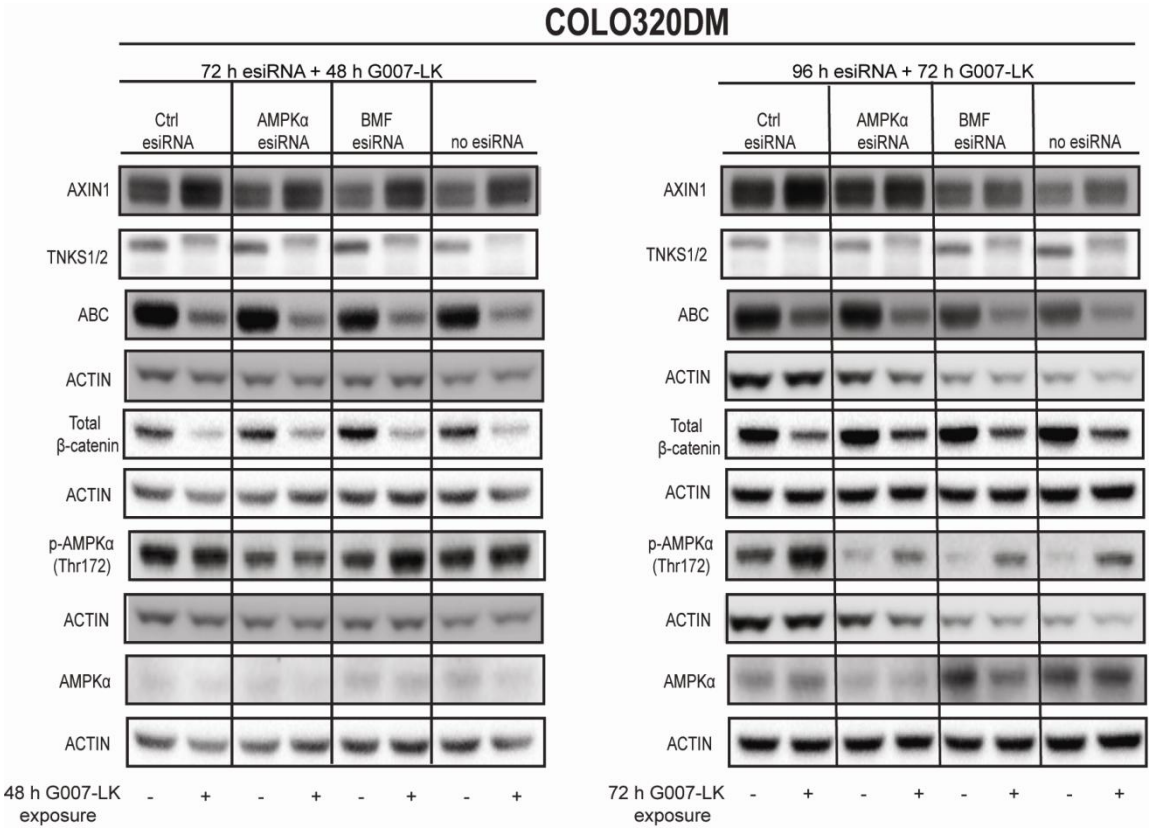


**Figure 3-4B:** The WB analysis represents that G007-LK exposure in COLO320DM led to the following: i) Increased AXIN1 expression. ii) Decreased TNKS1/2 and ABC expression. iii) p-AMPKα (Thr172) levels were increased upon 72 h of G007-LK exposure. The cells were treated with [25 nM *AMPKα1* + 25nM *AMPKα2* (*AMPKα* )]esiRNA , 50 nM *BMF* esiRNA, 50 nM control (Ctrl) esiRNA or no esiRNA and vehicle (10% transfection buffer, 0.4% Pepmute and cell culture medium) for 24 h. The transfection was followed by 1 µM G007-LK treatment or vehicle (0.01% DMSO) for the last 48 h or 72 h. Cytoplasmic fractions extracted from COLO320DM were analyzed by WB using antibodies against AXIN1, TNKS1/2, ABC, total β-catenin, p-AMPKα (Thr172), AMPKα and ACTIN (loading control).

# 4. Discussion

The project aimed to validate if the cancer cell lines ABC-1, OVCAR-4, A498, COLO320DM and SW480 are G007-LK-sensitive. G007-LK-sensitive cell lines may display at least one of the following features: i) TNKS1/2 inhibition (usually observed as differently expressed TNKS1/2 protein levels). ii) Increased AXIN protein levels. iii) Decreased WNT pathway signaling and iv) Reduced proliferation [4]. Furthermore, the aim was also to explore BMF as a potential biomarker in response to G007-LK treatment, and investigate a potential interplay between AXIN, AMPK and BMF.

## 4.1 G007-LK sensitive cancer cell lines

G007-LK-sensitive cancer cell lines have initially been defined by growth reduction due to an inhibition of the WNT pathway [4]. In this scenario, TNKS1/2 inhibition stabilizes the rate limiting structural protein AXIN in the β-catenin degradation complex [4][3]. This leads to a higher turnover of β-catenin which is N-terminal phsophorylated by CK1γ and GSK3β, followed by a polyubiquitination through β-TRCP and finally its degradation in the 26S proteasome [12].

However, sensitivity to tankyrase inhibition may not necessarily lead to altered growth. Instead, broad spectrums of possible responses have been described. Some tumor cell lines show AXIN stabilization followed by reduced β-catenin levels upon tankyrase inhibition, but no altered growth. Indeed, some of the most sensitive cell lines to tankyrase inhibition show no alterations in the WNT pathway [4]. As a consequence, it has been difficult to find good biomarkers that would predict response to tankyrase inhibitor G007-LK treatment.

We selected 5 diverse tumor cell lines that were sensitive to G007-LK from a broad search for G007-LK-sensitive cell lines as defined by growth inhibition. In this study ABC-1, COLO320DM, OVCAR-4 and SW480 exhibited significant growth inhibition upon G007-LK exposure (Fig. 3-1). However, A-498 cells did not display statistically significant growth inhibition upon G007-LK treatment (Fig. 3-1, C). ABC-1 cells are also being tested in immunodeficient mice xenograft assays for G007-LK treatment response.

All the tested cell lines in this thesis displayed at least one of the following features: i) TNKS1/2 inhibition. ii) Increased AXIN protein levels iii) Decreased WNT pathway signaling iv) Reduced proliferation. According to the above mentioned G007-LK-sensitive cancer cell line criteria, all the tested cancer cell lines in this thesis were validated to be G007-LK-sensitive (Fig. 3-1, 3-2A, 3-2B and 3-4B).

SW480, OVCAR-4, A-498, ABC-1 and COLO320DM displayed TNKS1/2 inhibition and AXIN1 stabilization upon 72 h of G007-LK treatment (Fig. 3-2B and 3-4B). A previous study found COLO320DM and SW480 displaying TNKS1/2 inhibition and AXIN2 protein stabilization upon TNKS1/2 inhibitor treatment [4]. Another TNKS1/2 inhibitor, XAV939,

stabilizes both AXIN protein levels upon TNKS1/2 inhibition in the SW480 cancer cell line [3]. In this research, we demonstrate that the TNKS1/2 inhibitor G007-LK stabilizes AXIN1 protein upon TNKS1/2 inhibition *in vitro* (Fig. 3-2B and 3-4B).

Furthermore, SW480 and COLO320DM displayed down-regulation of *AXIN2* transcripts and inhibition of ABC and total β-catenin upon G007-LK exposure (Fig. 3-2A, 3-2B and 3-4B). It is known that AXIN proteins are the main rate limiting aspect of the β-catenin DC. *AXIN1* is produced continuously, but *AXIN2* is a WNT pathway target gene and forms a negative feedback loop for WNT pathway regulation [77]. Downregulation of *AXIN2* mRNA transcription indicates WNT pathway inhibition [77][78]. Since accumulated cytosolic non-phosphorylated active form of β-catenin (ABC) may translocate to the nucleus, and nuclear β-catenin along with TCF/LEF may initiate transcription of the WNT pathway target genes, decrease of cytosolic ABC also indicates WNT pathway inhibition [5][12]. Since SW480 and COLO320DM displayed downregulation of *AXIN2* transcripts and decrease of ABC and total β-catenin protein levels, they are sensitive to WNT pathway inhibition upon G007-LK exposure (Fig. 3-2A, 3-2B and 3-4B). Lau et al. found COLO320DM to be WNT pathway inhibition sensitive but not SW480. Lau et al. claimed that SW480 does not exhibit inhibition of WNT pathway target gene by TNKS1/2 inhibitors [4]. However, JW74 (G007-LK analogue) has been proven to cause inhibition of WNT pathway target gene in SW480 [48].

Interestingly, OVCAR-4 displayed inhibition of *AXIN2* mRNA but increase in the cytoplasmic ABC levels upon 72 h of G007-LK exposure (Fig. 3-2A and 3-2B). Oppositely, ABC-1 displayed a mild to moderate upregulation of *AXIN2* mRNA but a moderate decrease in cytoplasmic ABC upon 72 h of G007-LK treatment (Fig. 3-2A, 3-2B and 3-3B). It is important to mention here that the WNT pathway is not a sole regulator of β-catenin and β-catenin/TCF mediated transcription [79]. Other pathways may influence β-catenin and β-catenin/TCF mediated transcription: i) Protein kinase A (PKA) may phosphorylate β-catenin at Ser 675 and save it from proteolysis [79]. ii) E-cadherin bound β-catenin serves in the formation of cell-cell adherens junctions [80]. Activated G protein, $G_{12}$, may unbound β-catenin from E-cadherin [79]. Thus, free β-catenin accumulates and its translocation to the nucleus mediates β-catenin/TCF transcription [79][80]. iii) Insulin/insulin-like growth factor 1 pathway may influence the β-catenin/TCF mediated transcription. The WNT pathway target genes *C-MYC* and *CYCLIN D1* are upregulated upon insulin stimulation through protein kinase B(PKB)-dependent and PKB-independent mechanisms [81][79]. Therefore, there may be other factors involved causing cytoplasmic ABC stabilization in OVCAR-4 and cytoplasmic ABC downregulation in ABC-1 upon G007-LK treatment (Fig. 3-2B, 3-3B).

## 4.2 Is BMF a biomarker in response to G007-LK treatment in the cancer cell lines?

*BMF* transcriptional upregulation was observed in response to G007-LK treatment in the cancer cell lines SW480, COLO320DM, ABC-1 and OVCAR-4 (Fig. 3-2A). In the most G007-LK-growth-inhibition-sensitive cell lines ABC-1 and COLO320DM (Fig. 3-1, A and B), the increase of *BMF* mRNA was particular strong. We do not know whether the increased presence of *BMF* transcripts translated into higher amounts of BMF protein due to the challenging nature of reliable protein detection in WB analysis. For instance, *BMF* mRNA upregulation was observed but BMF protein levels could not be verified in the MCF-10A cells by Schmelzle and team due to poor available antibodies against BMF [70]. Despite these technical difficulties we find the significant upregulation of *BMF* mRNA an encouraging step towards defining *BMF* transcripts as a biomarker for tankyrase inhibition in cancer cells. More work on a broader range of G007-LK-sensitive and G007-LK-insensitive tumor cell lines will be required to establish how predictive BMF is for reduced tumor cell proliferation upon G007-LK treatment.

We aim to test more antibodies against BMF protein in the future. Other methods such as targeted mass spectrometry and stable isotope labeling by amino acids in cell culture (SILAC) can also reliably quantify proteins. Our group has prepared samples to be run for SILAC to detect BMF protein levels in the G007-LK treated cells.

## 4.3 Interplay between AXIN1, AMPK and *BMF* upon treatment with TNKS1/2 inhibitor G007-LK

Our work establishes *BMF* transcriptional upregulation upon G007-LK exposure in a number of cancer cell lines (Fig. 3-2A). The AMPK-activation pathway was chosen to explore a potential interplay between AXIN1, AMPK and *BMF* upon treatment with G007-LK, because we found strong potential links between AXIN, AMPK activation and BMF in literature [4][6][72].
Apart from being the key regulator of cell metabolism [7], AMPK is also involved in cell polarity and cell growth maintenance [71]. AMPK is a heterodimer that consists of the α-catalytic subunit, β and γ-regulatory subunits. AMPK is activated upon phosphorylation of theronine (Thr)-172 at the α-catalytic subunit by the kinase complex: Liver kinase B1(LKB1)-STE20-related kinase adapter protein (STRAD)-mouse protein 25 (MO25)[7].

An interesting functional finding of this study is the affect of G007-LK-mediated AXIN1 stabilization on AMPK phosphorylation in COLO320DM but not in ABC-1 tumor cells as detected by a p-AMPKα (Thr172) specific antibody (Fig. 3-4B, right). It is important to note here that LKB-1 is the prime AMPK activation kinase [82][83] and mutations in LKB-1 will affect AMPK activation [83]. ABC-1 is a lung cancer cell line. The *LKB-1/Serine/threonine kinase 11(STK11)* gene is known to be mutated in lung cancers [84] and it is therefore

tempting to speculate that LKB-1 may be involved in the observed differential phosphorylation of AMPK (at Thr172) in COLO320DM cells, but not in ABC-1 cells. Effects of *LKB-1/STK11* must also be explored in both COLO320DM and ABC-1 in further studies.

# 5. Conclusion

ABC-1, COLO320DM, OVCAR-4, A-498 and SW480 were validated to be G007-LK-sensitive cancer cell lines (Fig. 3-1, 3-2A, 3-2B and 3-4B). Furthermore, we established *BMF* transcripts as potentially broader biomarkers for TNKS1/2 inhibition in cancer cells compared to the previously used β-catenin biomarker (Fig. 3-2A, Fig. 3-2B). We also show a regulatory interaction between *BMF* depletion and AMPKα in COLO320DM that depends on TNKS1/2 inhibitor G007-LK activity (Fig. 3-4B, right). We finally demonstrate that AMPK phosphorylation (at Thr172) is increased by G007-LK-mediated TNKS1/2 inhibition, perhaps through AXIN1 stabilization, in COLO320DM (Fig. 3-4B, right).

# References


[1] T. Haikarainen, S. Krauss, and L. Lehtiö, "Tankyrases: Structure , Function and Therapeutic Implications in Cancer," pp. 6472–6488, 2014.

[2] J. L. Riffell, C. J. Lord, and A. Ashworth, "Tankyrase-targeted therapeutics: expanding opportunities in the PARP family," *Nat Rev Drug Discov*, vol. 11, pp. 923–936, 2012.

[3] S.-M. A. Huang, Y. M. Mishina, S. Liu, A. Cheung, F. Stegmeier, G. A. Michaud, O. Charlat, E. Wiellette, Y. Zhang, S. Wiessner, M. Hild, X. Shi, C. J. Wilson, C. Mickanin, V. Myer, A. Fazal, R. Tomlinson, F. Serluca, W. Shao, H. Cheng, M. Shultz, C. Rau, M. Schirle, J. Schlegl, S. Ghidelli, S. Fawell, C. Lu, D. Curtis, M. W. Kirschner, C. Lengauer, P. M. Finan, J. A. Tallarico, T. Bouwmeester, J. A. Porter, A. Bauer, and F. Cong, "Tankyrase inhibition stabilizes axin and antagonizes Wnt signalling.," *Nature*, vol. 461, pp. 614–620, 2009.

[4] T. Lau, E. Chan, M. Callow, J. Waaler, J. Boggs, R. A. Blake, S. Magnuson, A. Sambrone, M. Schutten, R. Firestein, O. Machon, V. Korinek, E. Choo, D. Diaz, M. Merchant, P. Polakis, D. D. Holsworth, S. Krauss, and M. Costa, "A novel tankyrase small-molecule inhibitor suppresses APC mutation-driven colorectal tumor growth," *Cancer Res.*, vol. 73, pp. 3132–3144, 2013.

[5] A. Voronkov and S. Krauss, "Wnt/beta-catenin signaling and small molecule inhibitors.," *Curr. Pharm. Des.*, vol. 19, pp. 634–64, 2013.

[6] S. M. Kilbride, A. M. Farrelly, C. Bonner, M. W. Ward, K. C. Nyhan, C. G. Concannon, C. B. Wollheim, M. M. Byrne, and J. H. M. Prehn, "AMP-activated protein kinase mediates apoptosis in response to bioenergetic stress through activation of the pro-apoptotic Bcl-2 homology domain-3-only protein BMF," *J. Biol. Chem.*, vol. 285, pp. 36199–36206, 2010.

[7] B. Viollet, S. Horman, J. Leclerc, L. Lantier, M. Foretz, M. Billaud, S. Giri, and F. Andreelli, "AMPK inhibition in health and disease.," *Crit. Rev. Biochem. Mol. Biol.*, vol. 45, pp. 276–295, 2010.

[8] R. Nusse and H. Varmus, "Three decades of Wnts: a personal perspective on how a scientific field developed," *The EMBO Journal*, vol. 31. pp. 2670–2684, 2012.

[9] A. Kikuchi, H. Yamamoto, and A. Sato, "Selective activation mechanisms of Wnt signaling pathways," *Trends in Cell Biology*, vol. 19. pp. 119–129, 2009.

[10] M. Katoh, "WNT/PCP signaling pathway and human cancer (Review)," *Oncology Reports*, vol. 14. pp. 1583–1588, 2005.

[11] A. De, "Wnt/Ca2+ signaling pathway: a brief overview.," *Acta Biochim. Biophys. Sin. (Shanghai).*, vol. 43, pp. 745–56, 2011.

[12] B. T. MacDonald, K. Tamai, and X. He, "Wnt/β-Catenin Signaling: Components, Mechanisms, and Diseases," *Developmental Cell*, vol. 17. pp. 9–26, 2009.

[13] B. Alberts, A. Johnson, J. Lewis, M. Rafi, K. Roberts, and P. Walter, *Molecular Biology of the Cell (Fifth Edition)*, vol. 11. 2008, p. 1392.

[14] D. Kimelman and W. Xu, "beta-catenin destruction complex: insights and questions from a structural perspective.," *Oncogene*, vol. 25, pp. 7482–7491, 2006.

[15] J. Waaler, *Development of specific tankyrase inhibitors for attenuating canonical WNT/β-catenin signaling*. Ph D thesis 2013.

[16] X. Zeng, H. Huang, K. Tamai, X. Zhang, Y. Harada, C. Yokota, K. Almeida, J. Wang, B. Doble, J. Woodgett, A. Wynshaw-Boris, J.-C. Hsieh, and X. He, "Initiation of Wnt signaling: control of Wnt coreceptor Lrp6 phosphorylation/activation via frizzled, dishevelled and axin functions.," *Development*, vol. 135, pp. 367–375, 2008.

[17] B. T. MacDonald, C. Yokota, K. Tamai, X. Zeng, and X. He, "Wnt signal amplification via activity, cooperativity, and regulation of multiple intracellular PPPSP motifs in the Wnt co-receptor LRP6," *J. Biol. Chem.*, vol. 283, pp. 16115–16123, 2008.

[18] "The Wnt homepage/Nusselab," 2014. [Online]. Available: http://www.stanford.edu/group/nusselab/cgi-bin/wnt/target_genes.

[19] C. Y. Logan and R. Nusse, "The Wnt signaling pathway in development and disease.," *Annu. Rev. Cell Dev. Biol.*, vol. 20, pp. 781–810, 2004.

[20] R. H. Giles, J. H. Van Es, and H. Clevers, "Caught up in a Wnt storm: Wnt signaling in cancer," *Biochimica et Biophysica Acta - Reviews on Cancer*, vol. 1653. pp. 1–24, 2003.

[21] P. J. Morin, A. B. Sparks, V. Korinek, N. Barker, H. Clevers, B. Vogelstein, and K. W. Kinzler, "Activation of beta-catenin-Tcf signaling in colon cancer by mutations in beta-catenin or APC.," *Science*, vol. 275, pp. 1787–1790, 1997.

[22] H. Suzuki, D. N. Watkins, K.-W. Jair, K. E. Schuebel, S. D. Markowitz, W. D. Chen, T. P. Pretlow, B. Yang, Y. Akiyama, M. Van Engeland, M. Toyota, T. Tokino, Y. Hinoda, K. Imai, J. G. Herman, and S. B. Baylin, "Epigenetic inactivation of SFRP genes allows constitutive WNT signaling in colorectal cancer.," *Nat. Genet.*, vol. 36, pp. 417–422, 2004.

[23] O. Aguilera, M. F. Fraga, E. Ballestar, M. F. Paz, M. Herranz, J. Espada, J. M. García, A. Muñoz, M. Esteller, and J. M. González-Sancho, "Epigenetic inactivation of the Wnt antagonist DICKKOPF-1 (DKK-1) gene in human colorectal cancer.," *Oncogene*, vol. 25, pp. 4116–4121, 2006.

[24] J. Mazieres, B. He, L. You, Z. Xu, A. Y. Lee, I. Mikami, N. Reguart, R. Rosell, F. McCormick, and D. M. Jablons, "Wnt inhibitory factor-1 is silenced by promoter hypermethylation in human lung cancer," *Cancer Res.*, vol. 64, pp. 4717–4720, 2004.

[25] P. Polakis, “The many ways of Wnt in cancer,” *Current Opinion in Genetics and Development*, vol. 17. pp. 45–51, 2007.

[26] N. Barker and H. Clevers, “Mining the Wnt pathway for cancer therapeutics.,” *Nat. Rev. Drug Discov.*, vol. 5, pp. 997–1014, 2006.

[27] C. Niehrs and S. P. Acebron, “Mitotic and mitogenic Wnt signalling,” *The EMBO Journal*, vol. 31. pp. 2705–2713, 2012.

[28] L. Hartwell, L. Hood, M. L. Goldberg, A. Reynolds, and L. M. Silver, *Genetics: from genes to genomes*, vol. 422. 2006, p. 887.

[29] A. Murray, “Cell cycle checkpoints,” *Current Opinion in Cell Biology*, vol. 6. pp. 872–876, 1994.

[30] T. C. He, A. B. Sparks, C. Rago, H. Hermeking, L. Zawel, L. T. da Costa, P. J. Morin, B. Vogelstein, and K. W. Kinzler, “Identification of c-MYC as a target of the APC pathway.,” *Science*, vol. 281, pp. 1509–1512, 1998.

[31] J. I. Daksis, R. Y. Lu, L. M. Facchini, W. W. Marhin, and L. J. Penn, “Myc induces cyclin D1 expression in the absence of de novo protein synthesis and links mitogen-stimulated signal transduction to the cell cycle.,” *Oncogene*, vol. 9, pp. 3635–3645, 1994.

[32] A. L. Gartel, X. Ye, E. Goufman, P. Shianov, N. Hay, F. Najmabadi, and A. L. Tyner, “Myc represses the p21(WAF1/CIP1) promoter and interacts with Sp1/Sp3.,” *Proc. Natl. Acad. Sci. U. S. A.*, vol. 98, pp. 4510–4515, 2001.

[33] O. Tetsu and F. McCormick, “Beta-catenin regulates expression of cyclin D1 in colon carcinoma cells.,” *Nature*, vol. 398, pp. 422–426, 1999.

[34] R. Fodde, J. Kuipers, C. Rosenberg, R. Smits, M. Kielman, C. Gaspar, J. H. van Es, C. Breukel, J. Wiegant, R. H. Giles, and H. Clevers, “Mutations in the APC tumour suppressor gene cause chromosomal instability.,” *Nat. Cell Biol.*, vol. 3, pp. 433–438, 2001.

[35] M. V Hadjihannas, M. Brückner, B. Jerchow, W. Birchmeier, W. Dietmaier, and J. Behrens, “Aberrant Wnt/beta-catenin signaling can induce chromosomal instability in colon cancer.,” *Proc. Natl. Acad. Sci. U. S. A.*, vol. 103, pp. 10747–10752, 2006.

[36] D. Olmeda, S. Castel, S. Vilaró, and A. Cano, “Beta-catenin regulation during the cell cycle: implications in G2/M and apoptosis.,” *Mol. Biol. Cell*, vol. 14, pp. 2844–2860, 2003.

[37] M. O. Hottiger, P. O. Hassa, B. Lüscher, H. Schüler, and F. Koch-Nolte, “Toward a unified nomenclature for mammalian ADP-ribosyltransferases,” *Trends in Biochemical Sciences*, vol. 35. pp. 208–219, 2010.

[38] H. Otto, P. A. Reche, F. Bazan, K. Dittmar, F. Haag, and F. Koch-Nolte, "In silico characterization of the family of PARP-like poly(ADP-ribosyl)transferases (pARTs).," *BMC Genomics*, vol. 6, p. 139, 2005.

[39] L. Lehtiö, R. Collins, S. van den Berg, A. Johansson, L. G. Dahlgren, M. Hammarström, T. Helleday, L. Holmberg-Schiavone, T. Karlberg, and J. Weigelt, "Zinc Binding Catalytic Domain of Human Tankyrase 1," *J. Mol. Biol.*, vol. 379, pp. 136–145, 2008.

[40] T. Karlberg, N. Markova, I. Johansson, M. Hammarström, P. Schütz, J. Weigelt, and H. Schüler, "Structural basis for the interaction between tankyrase-2 and a potent Wnt-signaling inhibitor," *J. Med. Chem.*, vol. 53, pp. 5352–5355, 2010.

[41] C. E. Bell and D. Eisenberg, "Crystal structure of diphtheria toxin bound to nicotinamide adenine dinucleotide.," *Biochemistry*, vol. 35, pp. 1137–1149, 1996.

[42] L. Lehtiö, N. W. Chi, and S. Krauss, "Tankyrases as drug targets," *FEBS Journal*, vol. 280. pp. 3576–3593, 2013.

[43] S. J. Hsiao and S. Smith, "Tankyrase function at telomeres, spindle poles, and beyond," *Biochimie*, vol. 90. pp. 83–92, 2008.

[44] D. Slade, M. S. Dunstan, E. Barkauskaite, R. Weston, P. Lafite, N. Dixon, M. Ahel, D. Leys, and I. Ahel, "The structure and catalytic mechanism of a poly(ADP-ribose) glycohydrolase," *Nature*, vol. 477. pp. 616–620, 2011.

[45] R. G. James, K. C. Davidson, K. A. Bosch, T. L. Biechele, N. C. Robin, R. J. Taylor, M. B. Major, N. D. Camp, K. Fowler, T. J. Martins, and R. T. Moon, "WIKI4, a Novel Inhibitor of Tankyrase and Wnt/ß-Catenin Signaling," *PLoS One*, vol. 7, 2012.

[46] C. A. Kirby, A. Cheung, A. Fazal, M. D. Shultz, and T. Stams, "Structure of human tankyrase 1 in complex with small-molecule inhibitors PJ34 and XAV939," *Acta Crystallogr. Sect. F Struct. Biol. Cryst. Commun.*, vol. 68, pp. 115–118, 2012.

[47] J. Waaler, O. Machon, L. Tumova, H. Dinh, V. Korinek, S. R. Wilson, J. E. Paulsen, N. M. Pedersen, T. J. Eide, O. Machonova, D. Gradl, A. Voronkov, J. P. Von Kries, and S. Krauss, "A novel tankyrase inhibitor decreases canonical Wnt signaling in colon carcinoma cells and reduces tumor growth in conditional APC mutant mice," *Cancer Res.*, vol. 72, pp. 2822–2832, 2012.

[48] J. Waaler, O. Machon, J. P. Von Kries, S. R. Wilson, E. Lundenes, D. Wedlich, D. Gradl, J. E. Paulsen, O. Machonova, J. L. Dembinski, H. Dinh, and S. Krauss, "Novel synthetic antagonists of canonical Wnt signaling inhibit colorectal cancer cell growth," *Cancer Res.*, vol. 71, pp. 197–205, 2011.

[49] M. Narwal, H. Venkannagari, and L. Lehtiö, "Structural basis of selective inhibition of human tankyrases," *J. Med. Chem.*, vol. 55, pp. 1360–1367, 2012.

[50] H.-L. Guo, C. Zhang, Q. Liu, Q. Li, G. Lian, D. Wu, X. Li, W. Zhang, Y. Shen, Z. Ye, S.-Y. Lin, and S.-C. Lin, "The Axin/TNKS complex interacts with KIF3A and is

required for insulin-stimulated GLUT4 translocation," *Cell Research*, vol. 22. pp. 1246–1257, 2012.

[51] N. W. Chi and H. F. Lodish, "Tankyrase is a Golgi-associated mitogen-activated protein kinase substrate that interacts with IRAP in GLUT4 vesicles," *J. Biol. Chem.*, vol. 275, pp. 38437–38444, 2000.

[52] T. Y. J. Yeh, K. K. Beiswenger, P. Li, K. E. Bolin, R. M. Lee, T. S. Tsao, A. N. Murphy, A. L. Hevener, and N. W. Chi, "Hypermetabolism, hyperphagia, and reduced adiposity in tankyrase-deficient mice," *Diabetes*, vol. 58, pp. 2476–2485, 2009.

[53] T. A. Brown, *Genomes 3*, Third edit. Garland Science Publishing, 2007, p. 713.

[54] A. R. Moser, H. C. Pitot, and W. F. Dove, "A dominant mutation that predisposes to multiple intestinal neoplasia in the mouse.," *Science*, vol. 247, pp. 322–324, 1990.

[55] E. R. Fearon, "Molecular genetics of colorectal cancer.," *Annu. Rev. Pathol.*, vol. 6, pp. 479–507, 2011.

[56] E. W. Stratford, J. Daffinrud, E. Munthe, R. Castro, J. Waaler, S. Krauss, and O. Myklebost, "The tankyrase-specific inhibitor JW74 affects cell cycle progression and induces apoptosis and differentiation in osteosarcoma cell lines.," *Cancer Med.*, vol. 3, pp. 36–46, 2014.

[57] A. Voronkov, D. D. Holsworth, J. Waaler, S. R. Wilson, B. Ekblad, H. Perdreau-Dahl, H. Dinh, G. Drewes, C. Hopf, J. P. Morth, and S. Krauss, "Structural basis and SAR for G007-LK, a lead stage 1,2,4-triazole based specific tankyrase 1/2 inhibitor," *J. Med. Chem.*, vol. 56, pp. 3012–3023, 2013.

[58] P. Bouillet and A. Strasser, "BH3-only proteins - evolutionarily conserved proapoptotic Bcl-2 family members essential for initiating programmed cell death.," *J. Cell Sci.*, vol. 115, pp. 1567–1574, 2002.

[59] A. Shamas-Din, H. Brahmbhatt, B. Leber, and D. W. Andrews, "BH3-only proteins: Orchestrators of apoptosis," *Biochimica et Biophysica Acta - Molecular Cell Research*, vol. 1813. pp. 508–520, 2011.

[60] L. Coultas, B. E. Au, J. Beaumont, D. Au, and L. A. O. Reilly, "( 12 ) United States Patent," vol. 2, no. 12, pp. 5101–5107, 2009.

[61] H. Puthalakath, A. Villunger, L. A. O'Reilly, J. G. Beaumont, L. Coultas, R. E. Cheney, D. C. Huang, and A. Strasser, "Bmf: a proapoptotic BH3-only protein regulated by interaction with the myosin V actin motor complex, activated by anoikis.," *Science*, vol. 293, pp. 1829–1832, 2001.

[62] C. Smits, P. E. Czabotar, M. G. Hinds, and C. L. Day, "Structural Plasticity Underpins Promiscuous Binding of the Prosurvival Protein A1," *Structure*, vol. 16, pp. 818–829, 2008.

[63] A. R. Ramjaun, S. Tomlinson, A. Eddaoudi, and J. Downward, “Upregulation of two BH3-only proteins, Bmf and Bim, during TGF beta-induced apoptosis.,” *Oncogene*, vol. 26, pp. 970–981, 2007.

[64] Y. Zhang, M. Adachi, R. Kawamura, and K. Imai, “Bmf is a possible mediator in histone deacetylase inhibitors FK228 and CBHA-induced apoptosis.,” *Cell Death Differ.*, vol. 13, pp. 129–140, 2006.

[65] Z. Tianhu, Z. Shiguang, and L. Xinghan, “Bmf is upregulated by PS-341-mediated cell death of glioma cells through JNK phosphorylation,” *Mol. Biol. Rep.*, vol. 37, pp. 1211–1219, 2010.

[66] F. Grespi, C. Soratroi, G. Krumschnabel, B. Sohm, C. Ploner, S. Geley, L. Hengst, G. Häcker, and A. Villunger, “BH3-only protein Bmf mediates apoptosis upon inhibition of CAP-dependent protein synthesis.,” *Cell Death Differ.*, vol. 17, pp. 1672–1683, 2010.

[67] C. Moran, a Sanz-Rodriguez, a Jimenez-Pacheco, J. Martinez-Villareal, R. C. McKiernan, E. M. Jimenez-Mateos, C. Mooney, I. Woods, J. H. M. Prehn, D. C. Henshall, and T. Engel, “Bmf upregulation through the AMP-activated protein kinase pathway may protect the brain from seizure-induced cell death.,” *Cell Death Dis.*, vol. 4, p. e606, 2013.

[68] K. Lei and R. J. Davis, “JNK phosphorylation of Bim-related members of the Bcl2 family induces Bax-dependent apoptosis.,” *Proc. Natl. Acad. Sci. U. S. A.*, vol. 100, pp. 2432–2437, 2003.

[69] H. Wang, P. Maechler, K. A. Hagenfeldt, and C. B. Wollheim, “Dominant-negative suppression of HNF-1 α function results in defective insulin gene transcription and impaired metabolism – secretion coupling in a pancreatic β -cell line,” vol. 17, no. 22, pp. 6701–6713, 1998.

[70] T. Schmelzle, A. A. Mailleux, M. Overholtzer, J. S. Carroll, N. L. Solimini, E. S. Lightcap, O. P. Veiby, and J. S. Brugge, “Functional role and oncogene-regulated expression of the BH3-only factor Bmf in mammary epithelial anoikis and morphogenesis.,” *Proc. Natl. Acad. Sci. U. S. A.*, vol. 104, pp. 3787–3792, 2007.

[71] D. B. Shackelford and R. J. Shaw, “The LKB1-AMPK pathway: metabolism and growth control in tumour suppression.,” *Nat. Rev. Cancer*, vol. 9, pp. 563–575, 2009.

[72] Y. L. Zhang, H. Guo, C. S. Zhang, S. Y. Lin, Z. Yin, Y. Peng, H. Luo, Y. Shi, G. Lian, C. Zhang, M. Li, Z. Ye, J. Ye, J. Han, P. Li, J. W. Wu, and S. C. Lin, “AMP as a low-energy charge signal autonomously initiates assembly of axin-ampk-lkb1 complex for AMPK activation,” *Cell Metab.*, vol. 18, pp. 546–555, 2013.

[73] http://www.sigmaaldrich.com/life-science/functional-genomics-and-rnai/mission-esirna.html#mission_esirna.

[74] "MTS Promega." [Online]. Available: http://www.promega.com/products/cell-health-and-metabolism/cell-viability-assays/celltiter-96-aqueous-one-solution-cell-proliferation-assay-_mts_/. [Accessed: 10-Jan-2014].

[75] *https://www.lifetechnologies.com/no/en/home/life-science/pcr/real-time-pcr/qpcr-education/real-time-pcr-handbook.html*.

[76] "Overview of Protein electrophoresis." [Online]. Available: www.piercenet.com. [Accessed: 18-May-2014].

[77] E. Jho, T. Zhang, C. Domon, C.-K. Joo, J.-N. Freund, and F. Costantini, "Wnt/beta-catenin/Tcf signaling induces the transcription of Axin2, a negative regulator of the signaling pathway.," *Mol. Cell. Biol.*, vol. 22, pp. 1172–1183, 2002.

[78] J. Y. Leung, F. T. Kolligs, R. Wu, Y. Zhai, R. Kuick, S. Hanash, K. R. Cho, and E. R. Fearon, "Activation of AXIN2 expression by beta-catenin-T cell factor. A feedback repressor pathway regulating Wnt signaling.," *J. Biol. Chem.*, vol. 277, no. 24, pp. 21657–65, Jun. 2002.

[79] T. Jin, I. George Fantus, and J. Sun, "Wnt and beyond Wnt: Multiple mechanisms control the transcriptional property of β-catenin," *Cellular Signalling*, vol. 20. pp. 1697–1704, 2008.

[80] T. Valenta, G. Hausmann, and K. Basler, "The many faces and functions of β-catenin," *The EMBO Journal*, vol. 31. pp. 2714–2736, 2012.

[81] J. Sun and T. Jin, "Both Wnt and mTOR signaling pathways are involved in insulin-stimulated proto-oncogene expression in intestinal cells," *Cell. Signal.*, vol. 20, pp. 219–229, 2008.

[82] A. Woods, S. R. Johnstone, K. Dickerson, F. C. Leiper, L. G. D. Fryer, D. Neumann, U. Schlattner, T. Wallimann, M. Carlson, and D. Carling, "LKB1 Is the Upstream Kinase in the AMP-Activated Protein Kinase Cascade," *Curr. Biol.*, vol. 13, pp. 2004–2008, 2003.

[83] R. J. Shaw, M. Kosmatka, N. Bardeesy, R. L. Hurley, L. A. Witters, R. A. DePinho, and L. C. Cantley, "The tumor suppressor LKB1 kinase directly activates AMP-activated kinase and regulates apoptosis in response to energy stress.," *Proc. Natl. Acad. Sci. U. S. A.*, vol. 101, pp. 3329–3335, 2004.

[84] M. Sanchez-Cespedes, P. Parrella, M. Esteller, S. Nomoto, B. Trink, J. M. Engles, W. H. Westra, J. G. Herman, and D. Sidransky, "Inactivation of LKB1/STK11 is a common event in adenocarcinomas of the lung," *Cancer Res.*, vol. 62, pp. 3659–3662, 2002.

# Appendix 1: Abbreviations

| | |
|---|---|
| A1 | BCL2-related protein |
| ABC | non-phosphorylated active β-catenin |
| Abs | absorbance |
| ADP | adenosine diphosphate |
| AD | adenosine sub-site of tankyrase |
| AICAR | 5-aminoimidazole-4-carboxamide-1-beta-4-ribofuranoside |
| AMP | adenosine monophosphate |
| AMPK | adenosine monophosphate-activated protein kinase |
| AP-2 | activator protein |
| APC | adenomatous polyposis coli |
| $Apc^{Min}$ | Apc multiple intestinal neoplasia |
| ARC | ankyrin repeat cluster |
| ART | ADP-ribosyltransferase |
| ARTD | Diphtheria toxin-like ADP-ribosyltransferase |
| ATCC | American type culture collection |
| ATP | adenosine triphosphate |
| ATPase | adenosine triphosphate-ase |
| AXIN1 | axis inhibition protein 1 |
| AXIN2 | axis inhibition protein 2 |
| AXIN | axis inhibition protein 1 or 2 |
| BAK | BCL2-antagonist/killer 1 |
| BAX | BCL2-like protein 4 |
| BCL2 | B-cell lymphoma 2 |
| BCL-W | BCL2-like-protein-2 |
| BCL-XL | BCL-extra large |
| BH | BCL-2 homology domain |
| BMF | BCL2-modifying factor |
| BSA | bovine serum albumin |
| β-Trcp | β-transducin-repeat-containing protein |
| CDK | cyclin-dependent kinase |
| cDNA | complementary deoxyribonucleic acid |
| CK1α | casein kinases 1α |
| C-MYC | v-myc myelocytomatosis viral oncogene homolog |
| C-JUN | jun proto-oncogene |
| $C_t$ | threshold cycle number |
| $C_{t\ GOI}{}^{S}$ | threshold cycle number of the gene of interest in the treated sample |
| $C_{t\ GOI}{}^{C}$ | threshold cycle number of the gene of interest in the untreated sample |
| $C_{t\ norm}{}^{S}$ | threshold cycle number of the GAPDH in the treated sample |
| $C_{t\ norm}{}^{C}$ | threshold cycle number of the GAPDH in the untreated sample |
| CYCLIN-D1 | cyclin D1 |
| CRC | colorectal cancer |
| CREB | cAMP response element-binding protein |
| DC | destruction complex |
| DKK1 | dickkopf-related protein |
| DLC2 | dynein light chain 2 |
| DMSO | dimethyl sulfoxide, |
| DNA | deoxyribonucleic acid |

| | |
|---|---|
| DN-$HNF_1A$ | dominant-negative sm6 mutant of $HNF_1A$ |
| dNTPs | deoxyribonucleotide triphosphate |
| DSH | Disheveled |
| DTP | developmental therapeutics program |
| DUB | deubiquitinating enzymes |
| ECL | enhanced chemiluminescent |
| EMEM | Eagle's minimum essential medium |
| esiRNA | endoribonuclease-prepared small interfering RNA |
| FBS | fetal bovine serum |
| FRET | fluorescent resonance energy transfer |
| FZD | frizzled |
| G1 | gap 1 of the cell cycle |
| G2 | gap 2 phase of the cell cycle |
| GAPDH | Glyceraldehyde phosphate dehydrogenase |
| GLUT4 | glucose transporter type 4 |
| GSK3β | glycogen synthase kinase 3β |
| h | hour |
| HDACi | histone deacetylase inhibitor |
| $HNF_1A$ | hepatocyte nuclear factor 1A |
| HPS | histidine-, proline- and serine-rich |
| HRP | horseradish peroxide |
| $IC_{50}$-value | half maximal inhibitory concentration |
| Int-1 | integration site 1 of the mouse mammary tumor virus |
| IRAP | insulin responsive aminopeptidase interleukin 1 receptor antagonist |
| JCRB | Japanese collection of research bioresources cell bank |
| JNK | C-JUN NH(2)-terminal kinase |
| K | Lysine |
| KIF3a | kinesin family member 3A |
| L-15 | Leibovitz's L-15 medium |
| LKB1 | liver kinase B1 |
| LRP5/6 | receptor low density lipoprotein receptor-related protein 5/6 |
| MARsylation | mono (ADP-ribose)sylation |
| MCL1 | Myeloid cell leukemia 1 |
| min | minutes |
| MO25 | mouse protein 25 |
| MODY3 | maturity-onset diabetes-of-the-young type 3 |
| mRNA | messenger ribonucleic acid |
| MS | mass spectrometry |
| MTS | 3-(4,5-dimethylthiazol-2-yl)-5-(3-carboxymethoxyphenyl)-2-(4-sulfophenyl)-2H-tetrazolium, inner salt |
| $NAD^+$ | nicotinamide adenine dinucleotide |
| NCI | National cancer institute |
| NCI-60 | the 60 human tumor cell lines selected by the National cancer institute |
| N-terminal | amino-terminal |
| NF-κB | nuclear factor kappa-light-chain-enhancer of activated B cells |
| NI | nicotinamide binding site |
| *NKD* | naked |
| NuMA | nuclear mitotic apparatus protein |
| OC | osteosarcoma |
| P | proline |

| | |
|---|---|
| p38 | mitogen-activated protein kinase |
| PAR | poly (ADP-ribose) |
| PARG | poly (ADP-ribose) glycohydrolase |
| PARP | poly (ADP-ribose) polymerase |
| PARsylate | poly (ADP-ribose)sylate |
| PBS | phosphate buffered saline |
| PCR | polymerase chain reaction |
| PMS | phenazine methosiphate |
| P/S | penicillin/streptomycin |
| PS341 | bortezomib |
| PVDF | polyvinylidene difluoride |
| RISC | RNA-induced silencing complex |
| RNA | ribonucleic acid |
| RNaseIII | ribonuclease III |
| RNF146 | ring finger protein 146 |
| RSPO | R-spondin |
| qRT-PCR | quantitative reverse transcription polymerase chain reaction |
| S | synthesis phase of the cell cycle |
| S | serine |
| SAM | sterile alpha motif |
| SAR | structure-activity relationship |
| SDS | Sodium dodecyl sulfate |
| SDS-PAGE | Sodium dodecyl sulfate-polyacrylamide gelelectrophoresis |
| SE | seizures |
| SFRP | secreted frizzled related proteins |
| siRNA | small interfering ribonucleic acid |
| SMAD4 | mothers against decapentaplegic homolog |
| SP1 | promoter-specific transcription factor |
| ST-d1EGFP | Super-Topflash destabilized enhanced green fluorescent protein |
| ST-LUC | Super-Topflash luciferase |
| STRAD | STE20-related kinase adapter protein |
| TBM | tankyrase binding motifs |
| TCF/LEF | T cell factor/lymphoid enhancer factor |
| TGF-β | transforming growth factor beta |
| Thr | theronine |
| TNKS | telomeric repeat factor (TRF1)-interacting ankyrin-related ADP-ribose polymerases, tankyrase |
| TNKS1/2 | TNKS1 and TNKS2 |
| TRF1 | telomeric repeat factor |
| Ub | ubiquitin |
| USPs | ubiquitin specific proteases |
| USP34 | ubiquitin specific protease 34 |
| WB | Western blot |
| wp | well-plate |
| WT- $HNF_1A$ | wild-type $HNF_1A$ |
| wg | Wingless |
| WNT | Wingless-type mammary tumor virus integration site |
| WNT pathway | The canonical WNT/β-catenin pathway |
| $\Delta\Delta C_t$ | Comparative quantification algorithms |

# Appendix 2: Materials, equipments and software

| Material | Producer | catalog number |
|---|---|---|
| **Cell culture** | | |
| Eagle's Minimum Essential Medium (EMEM) | LGC-standards | 30-2003 |
| Leibovitz's L-15 medium (1x) | Life technologies | 11415-049 |
| Mc Coy's 5A with L-Glutamine | ATCC | ATCC 30-2007 |
| RPM1-1640 medium with L-glutamine and NaHCO3 | Sigma-aldrich | R8758 |
| Penicillin-Streptomycin | Sigma life Science | P4333 |
| Trypsin EDTA | Sigma life Science | T3924 |
| Fetal bovine serum | Life Technologies (Invitrogen) | 10270-106 |
| 4-{5-[(E)-2-{4- (2-chlorophenyl)-5-[5-(methylsulfonyl)pyridin-2-yl]-4H-1,2,4-triazol-3yl}ethenyl]-1,3,4-oxadiazol-2-yl}benzonitrile (G007-LK) | TC-scientific | |
| 5-Aminoimidazole-4-carboxamide ribonucleotide (AICAR) | Sigma | A9978 |
| 6-[4-(2-Piperidin-1-ylethoxy) phenyl]-3-pyridin-4-ylpyrazolo[1,5-a]pyrimidine (Compound C) | Sigma | P5499 |
| Dulbeco's Modified Eagle medium (DMEM) high glucose, HEPES, no phenol red | Life technologies | 21063-029 |
| The CellTiter 96® $AQ_{ueous}$ Non-Radioactive Cell Proliferation Assay | Promega | G5421 |
| **Tranfection materials** | | |
| PepMute Plus siRNA | SignaGen laboratories | SL 100571-1 |
| PepMute transfection buffer (5X) | SignaGen laboratories | SL 100575 |
| **qRT-PCR** | | |
| GenEluteTM Mammalian Total RNA Miniprep Kit | Sigma Aldrich | RTN350 |
| SuperScript® VILO™ cDNA Synthesis Kit | Life technologies | 11754-050 |
| TaqMan Gene Expression | Life technologies | 4369510 |

| | | |
|---|---|---|
| Mastermix | | |
| **Western blotting** | | |
| Glycerol | Sigma | G5516 |
| Sodium dodecyl sulphate (SDS) | Sigma | L3771 |
| Bromophenol blue sodium salt | Sigma | B5525 |
| β-merkaptoethanol (2-Merkaptoethanol) | AppliChem | A1108,0100 |
| Sodium chloride (NaCl) | Sigma Aldrich | S3014 |
| Tris hydrochloride, HCl | Sigma Aldrich | RES3098T |
| Ethylenediaminetetraacetic acid (EDTA) | Sigma Aldrich | 431788 |
| IGEPAL CA-630 | Sigma Aldrich | I-3021 |
| Sodium Fluoride (NaF) | Sigma Aldrich | S1504 |
| Sodium orthovanadate ($Na_3VO_4$) | Sigma Aldrich | S6508 |
| Protease inhibitor cocktail tablets | Roche applied science | 4693124001 |
| Nonfat dried milk | AppliChem | A0830,0500 |
| Tris buffered saline tween (TBS-T) tablets | Medicago | 09-7510-100 |
| Trizma-base | Sigma | T1503 |
| Glysine | Sigma | G7126 |
| Nu-PAGE® Tris-Acetate SDS running buffer 20X | Life technologies | LA0041 |
| Nu-PAGE® MOPS SDS running buffer 20X | Life technologies | NP0001 |
| Nu-PAGE® Novex® 4-12% Bis-Tris Protein gels, 1.0 mm, 10 well | Life technologies | EA0375BOX |
| Nu-PAGE® Novex® 3-8% Tris-Acetate Protein gels, 1.0 mm, 10 well | Life technologies | NP0321BOX |
| RIPA lysis buffer 10X | Millipore | 20-188 |
| Dimethyl Sulfoxide (DMSO) | Sigma | D8418 |
| Developer and replenisher | Carestream Readymatic | 5023866 |
| Fixer and replenisher | Carestream Readymatic | 5023874 |
| Quick start™ Bradford 1X Dye Reagent | Bio-Rad | 500-0205 |
| BSA standard solution (2 mg/ml) | GE Healthcare Bio sciences | |
| ECL™ prime Western blotting detection reagent | GE Healthcare | RPN2236 |
| **Ladders** | | |
| PageRuler prestained protein ladder | Thermo Scientific | 26616 |
| HiMark Pre-stained Protein Standard | Life technologies | LC5699 |

| | | |
|---|---|---|
| Precision plus protein dual color standards | Bio Rad | 161-0374 |
| **Primary antibodies** | | |
| anti-ACTIN: Polyclonal rabbit IgG | Sigma-Aldrich | A2066 |
| anti-AMPKα: (F6), monoclonal mouse IgG2b | Cell signaling technology | 2793 |
| anti-AXIN1: (C76H11), monoclonal rabbit IgG | Cell signaling technology | 2087 |
| anti-LAMIN B1: Polyclonal rabbit IgG | Abcam | ab16048 |
| anti-non-phopho (active) β-catenin: (Ser33/37/Thr41)(D13A1), monoclonal rabbit IgG | Cell signaling technology | 8814 |
| anti-phospho-AMPKα: (Thr172) (40H9), monoclonal rabbit IgG | Cell signaling technology | 2535 |
| anti-Tankyrase- 1/2: (H-350), polyclonal rabbit IgG | Santa Cruz Biotechnology, INC. | sc-8337 |
| anti-USP34: Polyclonal rabbit IgG | Bethyl | A300-824A |
| anti-β-catenin: Monoclonal mouse IgG1 | BD Transduction Laboratories | 610153 |
| **Secondary antibodies** | | |
| Donkey anti-mouse IgG-HRP | Santa Cruz Biotechnology | sc-2314 |
| Donkey anti-rabbit IgG-horseradish peroxide (HRP) | Santa Cruz Biotechnology | sc-2313 |

| **MISSION esiRNA** | | | |
|---|---|---|---|
| **Gene symbol** | **NCBI RefSeq ID** | **Producer** | **Catalog number** |
| *PRKAA1, AMPKα1* | NM_206907 | Sigma-aldrich | EHU074041 |
| *PRKAA2, AMPKα2* | NM_006252 | Sigma-aldrich | EHU042081 |
| *BMF* | NM_001003940 | Sigma-aldrich | EHU140941 |
| *USP34* | NM_014709 | Sigma-aldrich | EHU033451 |
| *EGFP* | ---------- | Sigma-aldrich | EHUEGFP |

| **TaqMan® Gene Expression Assay** | | | | |
|---|---|---|---|---|
| **Gene name** | **Gene symbol** | **Entrez Gene ID** | **Producer** | **Catalog number** |
| Protein kinase, AMP-activated α1 catalytic subunit | *PRKAA1, AMPKα1* | 5562 | life technologies | Hs01562315 |

| | | | | |
|---|---|---|---|---|
| Protein kinase, AMP-activated, α2 catalytic subunit | *PRKAA2, AMPKα2* | 5563 | life technologies | Hs00178903 |
| Bcl2 modifying factor | *BMF* | 90427 | life technologies | Hs00372937 |
| Glyceraldehyde-3-phosphate dehydrogenase | *GAPDH* | 2597 | life technologies | Hs02758991 |
| Ubiquitin specific peptidase 34 | *USP34* | 9736 | life technologies | Hs00611330 |
| AXIN2 | *AXIN2* | 8313 | life technologies | Hs00610344 |

| **Instruments** | |
|---|---|
| Name | Producer |
| Microscope Axiovert 25 | Carl Zeiss |
| Automated Cell Counter TC 20 | BioRad |
| Incubator | Termaks |
| Incubator | Forma Scientific, Inc |
| NanoDrop 2000c | Thermo Scientific |
| Ultrospec 2100 pro UV/Visible | Amersham Biosciences |
| Centrifuge 5810 R | eppendorf AG |
| IncuCyte | ThermoFisher Scientific |
| FLUO star Omega | BMG Lab tech |
| Applied Biosystems ViiA7 real-time PCR system | Life technologies |
| Universal Hood II Molecular gel imaging cabinet | BioRad |
| Developer | AGFA-Healthcare |
| XCell SureLock™ electrophoresis cell | Invitrogen |
| Trans-Blot® SD semi-dry electrophoretic transfer cell | BioRad |
| Cyro freezing 1 ˚C container | NAGLENE™ |

| **Software** | |
|---|---|
| **Name** | **Producer** |
| Image J software version 1.47 | National Institutes of Health |
| ViiA7™ real-time PCR software version 1.2.2 | Life technologies |
| IncuCyte 2011A software | Essen Bio Science Inc. |
| SigmaPlot® 12.5 (Systat Software Inc.) | Systat Software Inc. |
| NanoDrop 2000c software | Thermo Scientific |

# Appendix 3: Buffers for SDS-PAGE and Western blot analysis

| **4 x Sample loading buffer:** | |
|---|---|
| (40% glycerol, 240 mM Tris/HCl pH 6.8, 8% SDS, 0.04% bromophenol blue, 5% β-merkaptoethanol) | **10 ml** |
| 100% glycerol | 4 ml |
| 1 M Tris/HCl pH 6.8 | 2.4 ml |
| SDS | 0.8 g |
| Bromophenol blue slurry | 4 mg |
| β-merkaptoetanol | 0.5 ml |
| Milli Q (MQ) $H_2O$ | 3.1 ml |
| Mix and store at 4˚C. | |
| | |
| **Cell lysis buffer** | |
| (10 mM Tris-HCl pH 7.4, 0.15 mM NaCl, 1 mM EDTA, 1% IGEPAL, 1 mM $Na_3VO_4$, 50m M NaF). | **500 ml** |
| 10 mM Tris/HCl | 0.61 g |
| 0.15 mM NaCl | 4.38 g |
| 1 mM EDTA | 1.86 g |
| 1% IGEPAL CA-630 | 5.00 g |
| NaF | 1.05 g |
| $Na_3VO_4$ | 0.09 g |
| Add 10 tablets of protease inhibitor cocktail. | |
| | |
| **Blocking buffer** | |
| (5% skimmed milk in 1xTBS-T) | **50 ml** |
| 5% skimmed milk powder | 25 g |
| 1xTBS-T | 50 ml |
| | |
| **10x protein transfer buffer** | |
| Trizma-base | 30.3 g |
| Glysin | 144.0 g |
| Add MQ $H_2O$ upto 1000 ml. | |
| Before use, add 200 ml methanol, 700ml MQ $H_2O$ to 100 ml of 10x protein transfer buffer. | |
| Before use, add 20% methanol, 70% MQ $H_2O$ and 10% 10x protein transfer buffer. | |
| | |
| **1xTBS-T pH 7.6** | |
| Dissolve 1 tablet of TBS-T in 500 ml of MQ $H_2O$. | |
| | |
| **Tris-acetate SDS running buffer** | |
| 20xTris-acetate SDS running buffer | 50 ml |
| $H_2O$ | 950 ml |
| | |

| **MOPS SDS running buffer** | |
|---|---|
| 20x MOPS SDS running buffer | 50 ml |
| $H_2O$ | 950 ml |
| | |
| **1xRIPA buffer** | |
| 10x RIPA | 10 ml |
| MQ $H_2O$ | 90 ml |
| | |

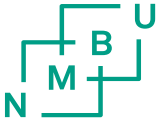

Norwegian University
of Life Sciences

Postboks 5003
NO-1432 Ås, Norway
+47 67 23 00 00
www.nmbu.no